JOURNAL OF PETROLOGY | VOLUME 50 | NUMBER 12 | PAGES 2345–2374 | 2009 | doi:10.1093/petrology/egp081

Magma Ascent along a Major Terrane Boundary: Crustal Contamination and Magma Mixing at the Drumadoon Intrusive Complex, Isle of Arran, Scotland

F. C. MEADE[1,2]*, D. M. CHEW[1,3], V. R. TROLL[1,4], R. M. ELLAM[5] AND L. M. PAGE[6]

[1]DEPARTMENT OF GEOLOGY, TRINITY COLLEGE DUBLIN, DUBLIN 2, IRELAND

[2]DEPARTMENT OF GEOGRAPHICAL AND EARTH SCIENCES, UNIVERSITY OF GLASGOW, GLASGOW G12 8QQ, UK

[3]DEPARTMENT OF EARTH SCIENCES, UNIVERSITY OF GENEVA, RUE DES MARAÎCHERS 13, 1205 GENEVA, SWITZERLAND

[4]DEPARTMENT OF EARTH SCIENCES, BERGGRUNDSGEOLOGI, UPPSALA UNIVERSITY, VILLAVÄGEN 16, SE-752 36 UPPSALA, SWEDEN

[5]SCOTTISH UNIVERSITIES ENVIRONMENTAL RESEARCH CENTRE, RANKINE AVENUE, EAST KILBRIDE, GLASGOW G75 OQF, UK

[6]DEPARTMENT OF GEOLOGY, LUND UNIVERSITY, SÖLVEGATAN 12, 223 62 LUND, SWEDEN

RECEIVED AUGUST 19, 2008; ACCEPTED NOVEMBER 4, 2009
ADVANCE ACCESS PUBLICATION DECEMBER 22, 2009

The composite intrusions of Drumadoon and An Cumhann crop out on the SE coast of the Isle of Arran, Scotland and form part of the larger British and Irish Palaeogene Igneous Province, a subset of the North Atlantic Igneous Province. The intrusions (shallow-level dykes and sills) comprise a central quartz–feldspar-phyric rhyolite flanked by xenocryst-bearing basaltic andesite, with an intermediate zone of dark quartz–feldspar-phyric dacite. New geochemical data provide information on the evolution of the component magmas and their relationships with each other, as well as their interaction with the crust through which they travelled. During shallow-crustal emplacement, the end-member magmas mixed. Isotopic evidence shows that both magmas were contaminated by the crust prior to mixing; the basaltic andesite magma preserves some evidence of contamination within the lower crust, whereas the rhyolite mainly records upper-crustal contamination. The Highland Boundary Fault divides Arran into two distinct terranes, the Neoproterozoic to Early Palaeozoic Grampian Terrane to the north and the Palaeozoic Midland Valley Terrane to the south. The Drumadoon Complex lies within the Midland Valley Terrane but its isotopic signatures indicate almost exclusive involvement of Grampian Terrane crust. Therefore, although the magmas originated at depth on the northern side of the Highland Boundary Fault, they have crossed this boundary during their evolution, probably just prior to emplacement.

KEY WORDS: *Arran; Palaeogene Igneous Province; crustal contamination; magma mixing; Sr isotopes; Nd isotopes; assimilation; Highland Boundary Fault*

INTRODUCTION

The North Atlantic Igneous Province

The North Atlantic Igneous Province (NAIP) stretches from Greenland to NW Britain and Ireland. The province

*Corresponding author. E-mail: meadef@tcd.ie and fiona.meade@ges.gla.ac.uk

has a total estimated area of $1{\cdot}3 \times 10^6$ km^2 and a volume of $(5–10) \times 10^6$ km^3 (White & McKenzie, 1989; Eldholm & Grue, 1994; Holbrook *et al.*, 2001). It developed in response to continental break-up of Euramerica, when the North American plate began to rift from the Eurasian plate as a result of the interaction of the Iceland mantle plume with the continental rift zones at ~60 Ma (Upton, 1988; Smallwood & White, 2002). The large head of a start-up mantle plume (see Richards *et al.*, 1989; Campbell & Griffiths, 1990) impacted on the base of the lithosphere and rapidly dispersed, causing initial magmatism over an area 2000 km in diameter (Phase 1). Magmatism then waned until ~56 Ma, when magma production increased as the lithosphere thinned and large-scale sea-floor spreading began (Phase 2) (Meyer *et al.*, 2007). The broad area initially influenced by the plume quickly reduced to a narrow core, *c.* 100 km in diameter (the plume tail), and magmatism focused on the spreading ridges, as seen today in Iceland and along the North Atlantic mid-ocean ridge (Storey *et al.*, 2007).

The British and Irish Palaeogene Igneous Province

The British and Irish Palaeogene Igneous Province (BIPIP) mostly formed during Phase 1 of the North Atlantic Igneous Province and comprises both lava fields and central complexes. It occurs at the southeasternmost extremity of the area influenced by the NAIP plume; igneous centres extend from St. Kilda in the north to Lundy in the south. The BIPIP has four main lava fields: Skye, Eigg and Mull in Scotland and Antrim in Northern Ireland. The Scottish lava fields are associated with, but pre-date the large central complexes of Skye, Rum and Mull (Emeleus & Bell, 2005).

The BIPIP, as part of the larger North Atlantic Igneous Province, is primarily a basaltic province and therefore large volumes of relatively pristine basaltic magma with mantle-like isotopic signatures are expected. However, the continental crust of the British and Irish segments of the NAIP is thick, fertile and variable in composition, and crustal contamination has proven to be a particularly important process in the formation of the more evolved magmas in the BIPIP (Dickin *et al.*, 1981, 1984; Kerr & Kempton, 1995; Geldmacher *et al.*, 1998, 2002; Troll *et al.*, 2004, 2005). The theory of crustal provincialism suggests that this variable crust has influenced the primary basaltic magmas, with crustal influences changing as terrane boundaries are traversed (Meighan, 1979; Dickin *et al.*, 1984; Meighan *et al.*, 1984; Thompson *et al.*, 1986; Gamble *et al.*, 1992; Geldmacher *et al.*, 1998, 2002; Kerr *et al.*, 1999). Hence, the magmas should be modified by the isotopic signature of the terrane through which they passed. In fact, Dickin *et al.* (1984) stated that 'the small degree of isotopic heterogeneity that may have been inherited from the mantle by the Tertiary [Palaeogene] magmas was far exceeded by the overwhelming influence of the continental crust'. Nowhere should this influence be more apparent than at the central volcanoes of the BIPIP, where long-lived magma storage and supply systems had time to develop, heating and assimilating the crust through repeated intrusion (Annen & Sparks, 2002; Troll *et al.*, 2004).

Whereas there are ~50 000 km^3 of mafic rocks within the province, there are only ~500 km^3 of felsic composition (Dickin *et al.*, 1984). Felsic rocks are almost exclusively associated with the central complexes, where they often form large granitic plutons or laccoliths (e.g. Skye, Arran and Mourne—Thompson, 1969; England, 1992; Stevenson *et al.*, 2007), micro-granite ring-dykes (e.g. Mull and Slieve Gullion—Emeleus, 1962; Sparks, 1988; McDonnell *et al.*, 2004) and thick sill complexes (e.g. Arran and Bute—Smellie, 1914; Harrison, 1925; Kanaris-Sotiriou & Gibb, 1985). At these central complexes magma suites are often bimodal in composition (basalt–rhyolite), whereas intermediate compositions are both spatially and volumetrically rare, a phenomenon known as the 'Bunsen–Daly gap' (Bunsen, 1851; Daly, 1925). This paucity of intermediate rocks has been a matter of debate for more than 150 years and a number of causes have been suggested. Besides the possibilities of sample bias and trapping of intermediate compositions at lower levels in the magma system, crustal contamination is believed to be the main process responsible for the formation of this magmatic gap (Dickin *et al.*, 1984; Marshall & Sparks, 1984; Geldmacher *et al.*, 1998).

The Isle of Arran

The Isle of Arran, in SW Scotland, was a site of intense igneous activity during the Palaeogene, and is bisected by a major crustal-scale discontinuity, the Highland Boundary Fault (Fig. 2). It thus affords the opportunity to investigate magmatism, magma transport mechanisms and crustal provincialism at a major terrane boundary. The Highland Boundary Fault represents the boundary between the Neoproterozoic to Early Palaeozoic Grampian Terrane to the north and the Palaeozoic Midland Valley Terrane to the south (Fig. 1) (Tanner, 2008).

Palaeogene igneous activity on Arran is focused in two main centres, the Northern Granite and the Central Complex (Fig. 3). Igneous activity is thought to have spanned ~4 Myr, from 61·7 to 57·4 Ma, based on palaeomagnetic constraints and geochronology. Palaeomagnetic studies place magmatism within chrons 26r, 26n and 25r (Hodgson *et al.*, 1990) and are supported by recent Ar–Ar radiometric dates for the Northern Granite ($57{\cdot}85 \pm 0{\cdot}15$ Ma; Chambers, 2000) and the Doon Sill ($58{\cdot}5 \pm 0{\cdot}8$ Ma; Mussett *et al.*, 1987). Magmatism on Arran shows a marked Bunsen–Daly gap, with large volumes of felsic magma represented by both the Northern Granite and the Central Complex (Dickin *et al.*, 1981). The Northern

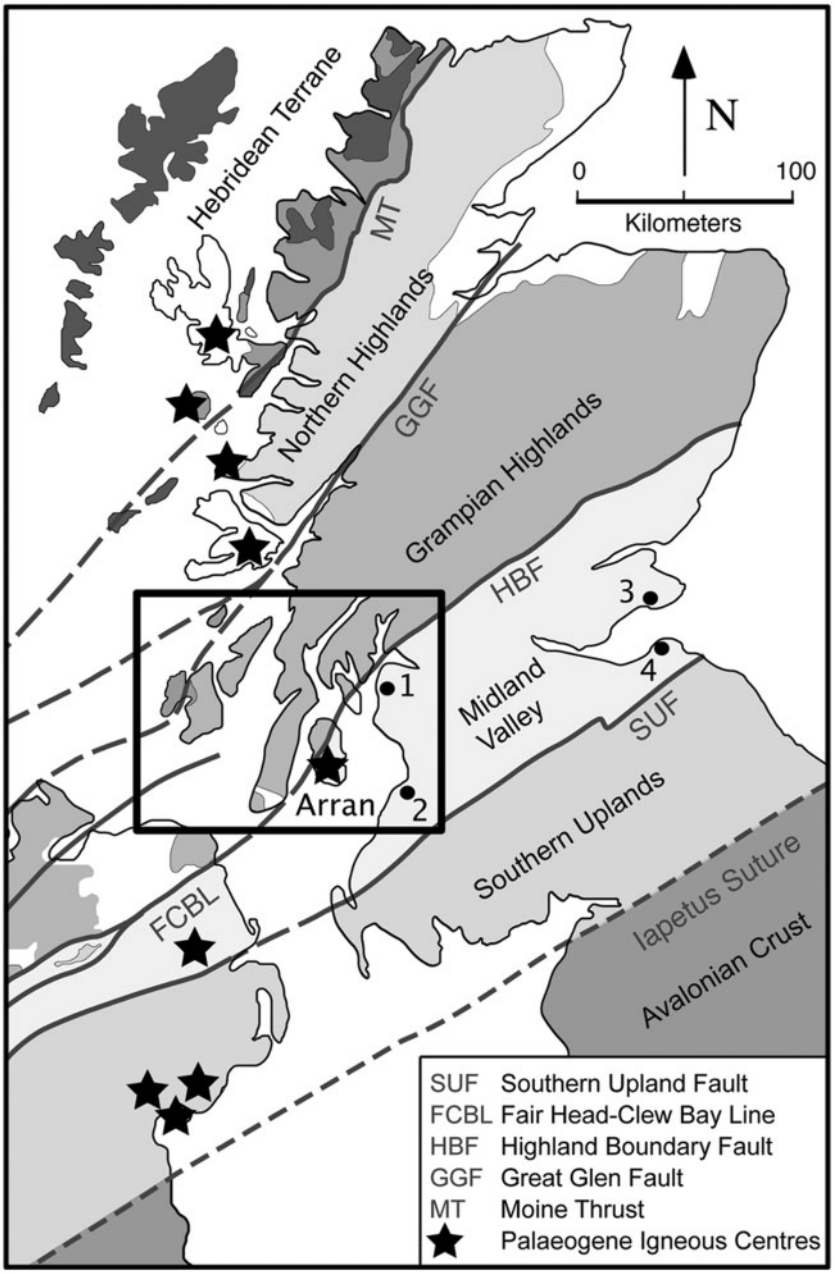

Fig. 1. Geological map of northern Britain and Ireland, showing the main basement terranes and terrane-bounding faults, modified after Chew (2003). The central volcanic complexes of the British and Irish Palaeogene Igneous province are marked with black stars. The Arran region is highlighted by a black rectangle as seen in detail in Fig. 2. Numbers 1–4 relate to the locations of vents containing xenoliths of Midland Valley Terrane basement. (1) Hawk's Nib, Holmbyre, Baidland Hill; (2) Heads of Ayr, Ashentree Glen, Dunaskin Glen; (3) Coalyard Hill; (4) Fidra, Briggs of Fidra, Partan Craig (after Halliday *et al.*, 1993).

Granite lies just north of the Highland Boundary Fault, whereas the Central Complex lies to the south of it. The Northern Granite is ~10 km in diameter and is composed of fine- and coarse-grained facies, both of which are biotite-bearing and drusy (England, 1992; Bell & Williamson, 2002). The Central Complex represents the high-level remnants of a deeply eroded caldera system, including both intrusive and extrusive rocks, ranging in composition from basalt to rhyolite (King, 1955; Bell & Williamson, 2002). Mafic magmas are represented both by minor intrusions and by larger bodies, which have been recognized at depth from geophysical data (Tantrigoda, 1999).

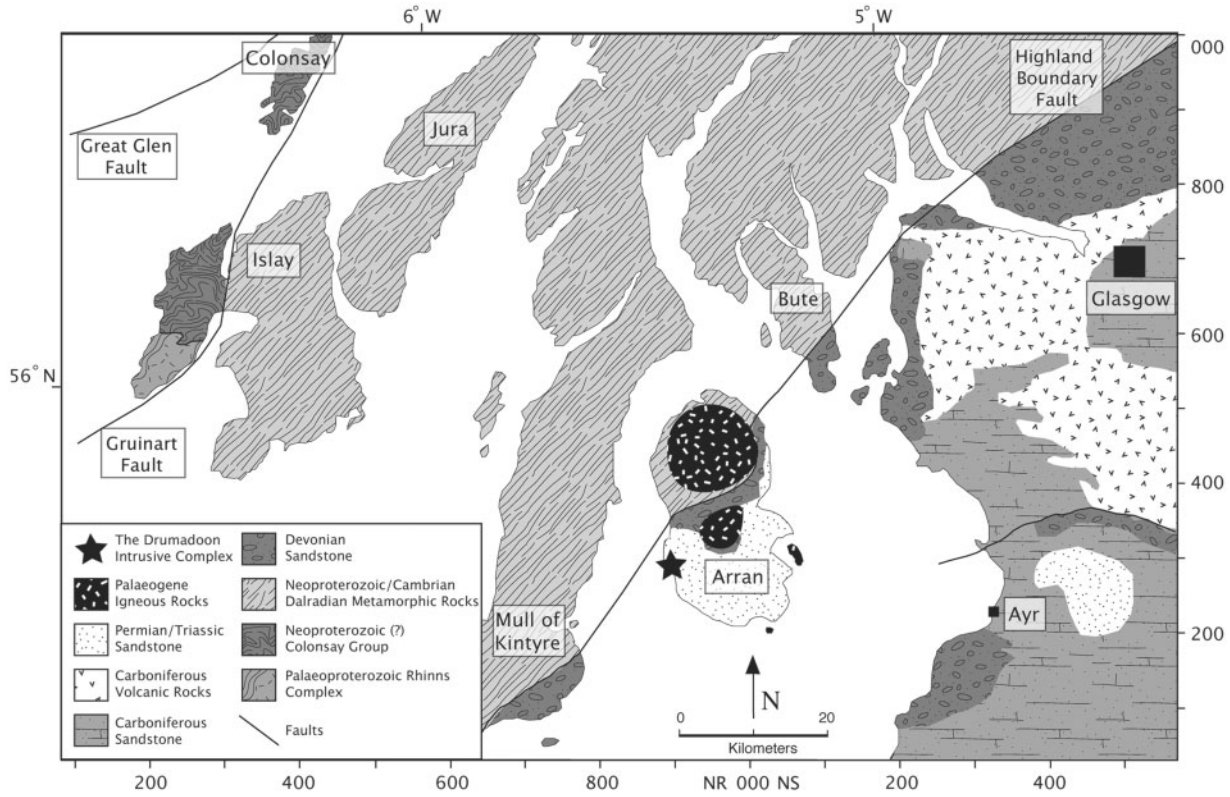

Fig. 2. Detailed geology of the Arran region, showing the Palaeoproterozoic to Early Palaeozoic Grampian Terrane to the north of the Highland Boundary Fault, and the Palaeozoic Midland Valley Terrane to the south. The main Palaeogene igneous centres on Arran are ornamented with a stippled black fill and the Drumadoon Intrusive Complex is marked with a black star. Similar intrusions to the Drumadoon Intrusive Complex are seen in southern Arran (see Fig. 3) and in the Midland Valley Terrane segment of the Isle of Bute, to the NE of Arran. Map modified after the British Geological Survey 1:625 000 bedrock geology UK north map (British Geological Survey, 2007) and figure 1.4 of Trewin & Rollin (2002). Longitude and latitude are marked on the top and left margins; local UK National Grid values (grid squares NR and NS) are marked on the bottom and right margins.

Late-stage alkaline magmatism formed riebeckite-bearing trachytes (Holy Island) and microgranites (Ailsa Craig) (Emeleus & Bell, 2005).

Arran is also characterized by several pulses of minor intrusions, including a well-developed regional north–south basaltic dyke swarm (Speight *et al.*, 1982). One of the more distinctive minor intrusive events comprises a series of quartz- and feldspar-phyric rhyolites. These rhyolites are seen both as large single intrusions (e.g. Brown Head) and as composite dykes and sills with basaltic andesite margins; for example, Drumadoon Point, the Doon Sill and Bennan Head (Judd, 1893; Harrison, 1925; Kanaris-Sotiriou & Gibb, 1985; Fig. 3). Petrologically, these intrusions have been considered to be part of the same intrusive event, examples of which are seen throughout Arran and the Isle of Bute (Smellie, 1914; Brown, 1929; Buist, 1952). Palaeomagnetic studies also suggest that these intrusions are members of the same phase of regional rhyolitic magmatism, related to a normal magnetic reversal, chron 26n (58·7–58·2 Ma) (Dagley *et al.*, 1978; Mussett *et al.*, 1987, 1989; Hodgson *et al.*, 1990; Gradstein *et al.*, 2004).

The Drumadoon Intrusive Complex

The Drumadoon Intrusive Complex in SE Arran is one such site of rhyolitic magmatism as described above. It lies ~8 km to the south of the Highland Boundary Fault within the Midland Valley Terrane (Figs 1–3). It comprises the composite intrusions (from north to south) of the An Cumhann Dyke, the Cleiteadh nan Sgarbh Dyke, the Doon Sill, the Drumadoon Point Sill and the Drumadoon Dyke (Figs 3 and 4). The dykes of Cleiteadh nan Sgarbh and An Cumhann are both ~30 m thick and generally comprise a central porphyritic rhyolite member flanked by a narrow (1–2 m) xenocryst-bearing basaltic andesite, often with a zone of porphyritic dacite between them. Work by Tyrrell (1928) and Kanaris-Sotiriou & Gibb (1985) considered these two outcrops to be part of the same intrusion and it is likely that they are feeders to the

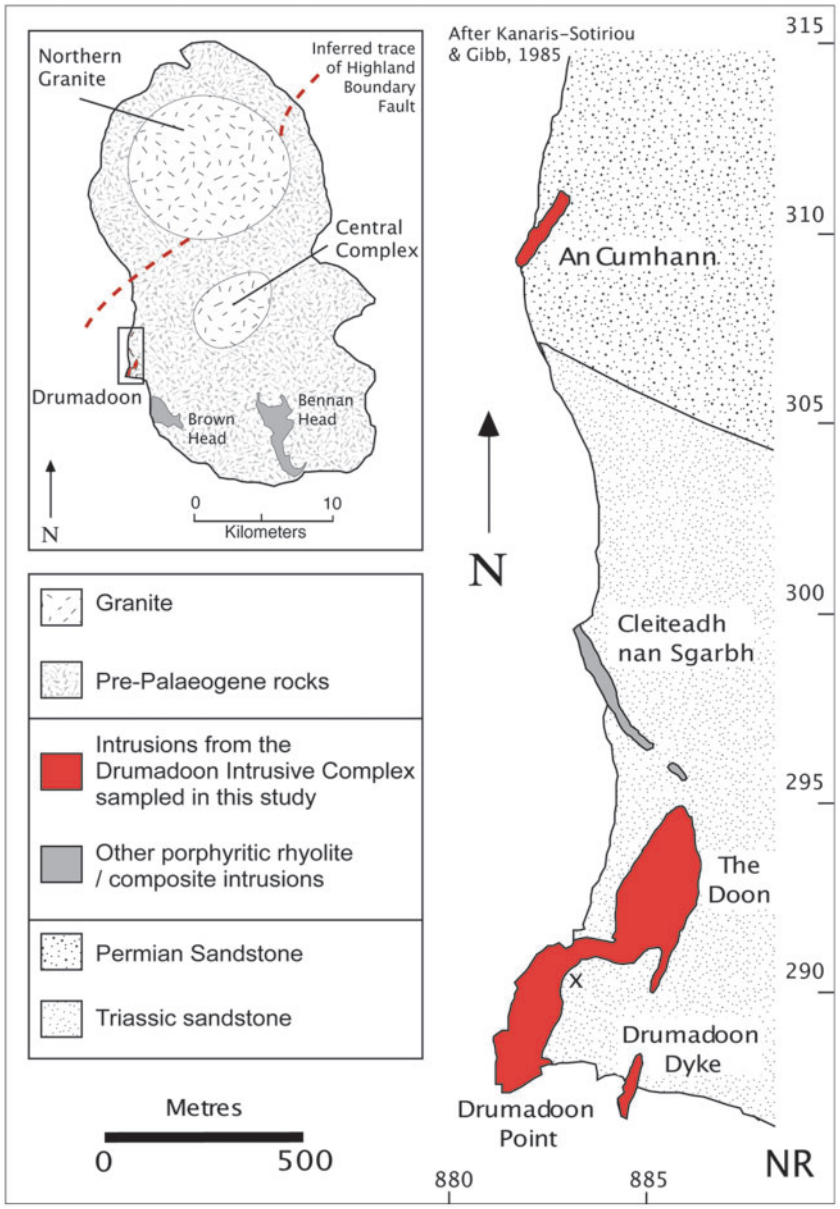

Fig. 3. Map of the Drumadoon Intrusive Complex (after Kanaris-Sotiriou & Gibb, 1985) with inset showing an overview of the porphyritic rhyolite sill complexes of Arran. X indicates the site where Fig. 4 was photographed. Grid labels are those of the UK National Grid. Grid square NR.

Doon–Drumadoon Point sill complex (MacDonald & Herriot, 1983).

The main Doon Sill and the lower-level sill at Drumadoon Point (which appear to be connected) predominantly comprise an enclave-bearing porphyritic rhyolite with narrow zones of dacite and xenocrystic basaltic andesite exposed at the margins of the intrusions. The Doon Sill is ~30 m thick, whereas the Drumadoon Point Sill crops out at sea level and its base is not seen. The upper part of the main Doon Sill is a quartz- and feldspar-phyric rhyolite that does not contain basaltic enclaves. In the case of the feeder dykes, this pristine quartz- and feldspar-phyric rhyolite fills the centre of the dykes, implying that it was the last magma to be intruded.

PETROLOGY AND PETROGRAPHY

Xenocrystic basaltic andesite

The xenocrystic basaltic andesites (Fig. 5a and b) range in grain size from medium- (dolerite) to fine-grained and have a matrix mostly composed of plagioclase laths and altered pyroxene, as well as some olivine. They contain

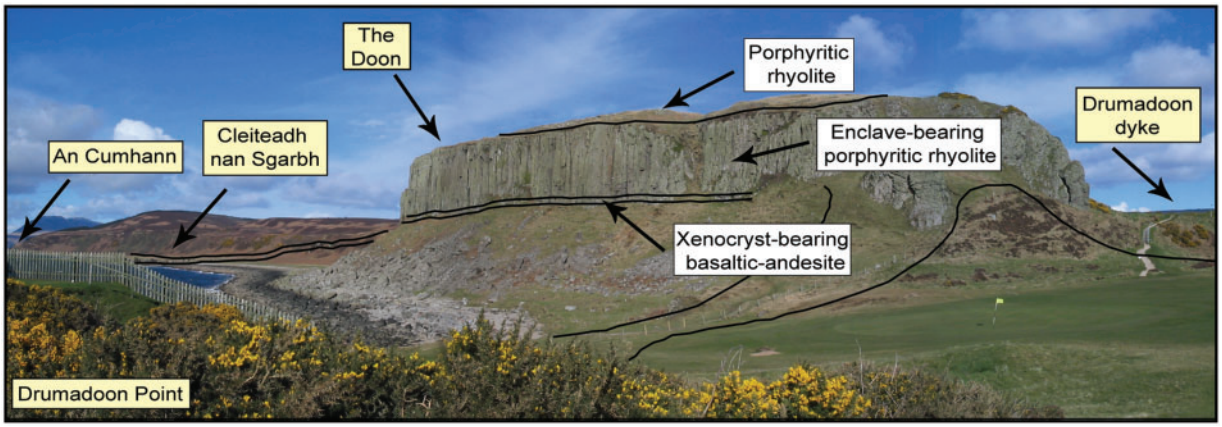

Fig. 4. Annotated photograph of the Drumadoon Intrusive Complex (looking NE). The Doon Sill is ~30 m thick. [See Fig. 3 for the location (X) from which the photograph was taken.]

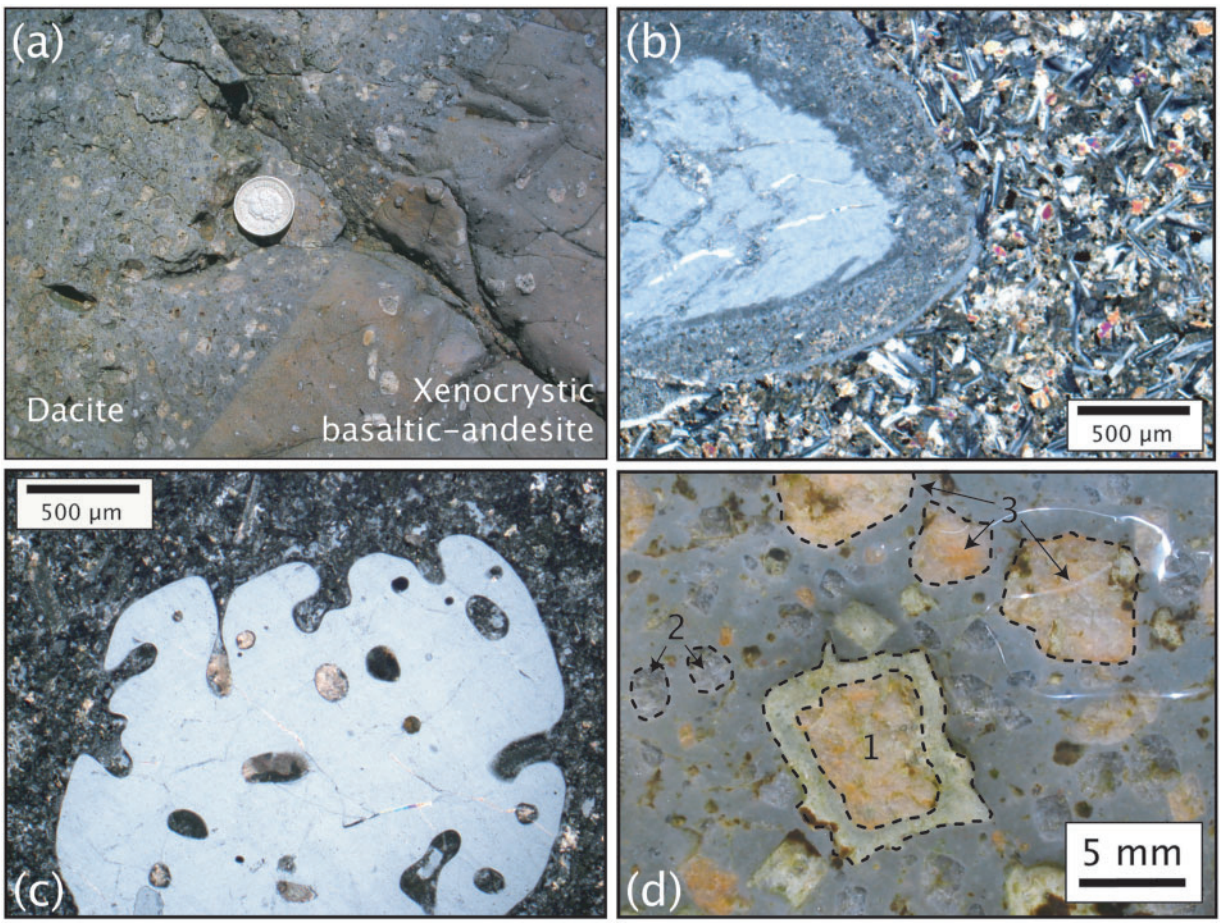

Fig. 5. (a) Field photograph showing basaltic andesite with xenocrysts of quartz and feldspar (bottom right). The basaltic andesite is in contact with a quartz- and feldspar-phyric dacite (top left). This contact is unchilled, though distinct. Coin for scale is 22 mm in diameter. (b) Thin-section photograph (in cross-polarized light; XPL) of a xenocrystic basaltic andesite, showing a feldspar xenocryst with an outer reaction rim. (c) Thin-section photograph (in XPL) of porphyritic dacite, showing a large embayed quartz crystal with a mainly quartz and feldspar matrix. (d) Field photograph of phenocrysts within the porphyritic rhyolite. Noteworthy features are a large, zoned, alkali feldspar with a plagioclase outer rim (1), smaller quartz phenocrysts (2), as well as alkali feldspar phenocrysts without obvious plagioclase rims (3).

~5% xenocrysts, mostly of embayed quartz (<3 mm) (60%) and rounded alkali feldspar (up to 8 mm in size) (40%). The feldspars have been heavily resorbed and show thin overgrowth rims (Fig. 5b). The matrix comprises 45% plagioclase laths, 5% opaque minerals and ~50% pyroxene, which has frequently been replaced by hornblende. Rounded groups of calcite crystals, surrounded by thin fine-grained rims, are also present. They most probably represent cross-sections through calcite amygdales that have grown within vesicles. The presence of vesicles in the basaltic andesite indicates that this dyke was intruded at high levels within the crust, most probably <3 km depth (see Paquet *et al.*, 2007, and references therein).

Porphyritic dacite

The porphyritic dacite (Fig. 5a and c) has a fine-grained matrix rich in feldspar. It contains ~10–20% phenocrysts, which include embayed quartz (up to 5 mm) (40%) and rounded, resorbed alkali feldspar phenocrysts (60%) up to ~10 mm in size. The dacite also contains ~2% unchilled basaltic andesite enclaves. Small millimetre-scale microenclaves and glomerocrysts of basaltic minerals are also seen within the matrix. There is a small amount of ferromagnesian minerals, showing alteration to amphibole.

Porphyritic rhyolite

The porphyritic rhyolite (Fig. 5d) has a fine-grained matrix of mostly feldspar with ~10% quartz. It contains ~35% phenocrysts, which include quartz (up to 5 mm and embayed in places) (25%), and zoned alkali feldspar (10–15 mm) (75%). The feldspar phenocrysts show resorbed edges in some cases; minor amounts of plagioclase are present.

Contact relationships

The internal contacts within the intrusions exhibit textures indicative of liquid–liquid interaction with no chilled margins (Fig. 6). Lobate contacts are common, as are enclaves of basaltic andesite within the rhyolite, and obvious phenocryst transfer between adjacent magmas (Fig. 6). A narrow zone of darker dacite often marks the contact between basaltic andesite and rhyolite, with an obvious, though unchilled, boundary with the basaltic andesite, grading inwards to a less obvious, lobate contact with the lighter-coloured rhyolite (Fig. 6). This dacite most probably represents the zone of interaction during intrusion, with the boundary with the basaltic andesite representing the mixing front (Fig. 5a). Entrained xenocrysts would not be expected beyond the limit of the mixing front if all interaction was occurring in the conduit. However, the basaltic andesite is nearly always xenocrystic, containing resorbed crystals of both quartz and K-feldspar (Fig. 5a and b). Assuming these crystals have been sourced from the rhyolite, this suggests that the basaltic andesite and rhyolite must also have interacted prior to intrusion. A rhyolitic source for the xenocrysts is supported by the mineral chemical data of Kanaris-Sotiriou & Gibb (1985) from the An Cumhann Dyke, whereby the alkali feldspars from both the rhyolite and basaltic andesite showed identical compositional ranges ($An_{22–30}$).

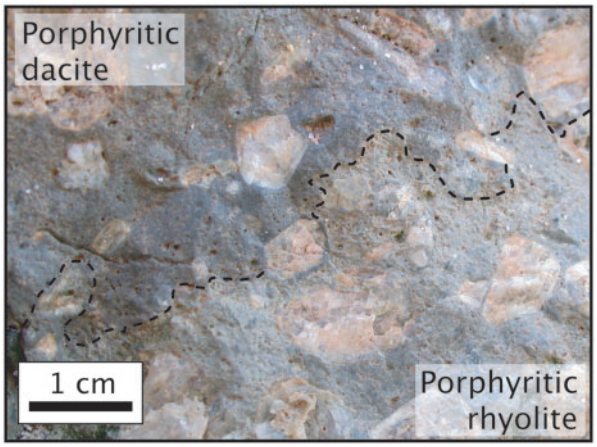

Fig. 6. Unchilled lobate contact between the porphyritic rhyolite and porphyritic dacite, recording apparent crystal transfer between the two magmas.

SAMPLE SELECTION AND PREPARATION

Samples of basaltic andesite, dacite, enclave-bearing rhyolite, and rhyolite from An Cumhann, the Doon Sill, Drumadoon Dyke and Drumadoon Point were analysed for major and trace elements and Sr and Nd isotopes, with the aim of elucidating the petrogenesis of these magmas, including quantification of their relationships with each other and also with the crust through which the magmas passed. These data allowed us to constrain the magma pathways along the major crustal discontinuity of the Highland Boundary Fault. Previous work by Dickin (1994), based on four samples from the Drumadoon suite, suggested the involvement of Grampian Terrane crust in the formation of the rhyolitic magmas. Kanaris-Sotiriou & Gibb (1985) analysed 44 samples (basaltic andesite and rhyolite) for major and trace elements by X-ray fluorescence (XRF). They did not consider a parental basic magma, but rather used the least evolved mafic sample as their mixing end-member. Our dataset ($n = 20$, Table 1) focuses on the Drumadoon Intrusive Complex with the intention of looking at crustal contamination and quantifying the involvement of varying crustal end-members, as well as having a more detailed look at magma mixing within the complex. Previously published

Table 1: Sample locations and lithological descriptions for samples from the Drumadoon Intrusive Complex

Sample no.	Lithological description and locality	Grid reference
DD-QFP-1	Enclave-bearing porphyritic dacite from fallen column from the Doon Sill	NR 88513 29350
DD-QFP-2	Porphyritic rhyolite from fallen column from the Doon Sill, no visible enclaves	NR 88494 29300
DD-QFP-3	Porphyritic rhyolite from fallen column from the Doon Sill	NR 88471 29183
DD-dQFP-4	Porphyritic dacite from northern edge of Drumadoon Point Sill	NR 88391 29105
DD-dQFP-5	Porphyritic dacite from northern edge of Drumadoon Point Sill	NR 88391 29108
DD-Dol-6	Xenocrystic basalt from base of the Doon Sill, 5 cm above base	NR 88482 29140
DD-Dol-8	Xenocrystic basaltic andesite from base of the Doon Sill, 5 cm above base	NR 88482 29140
DD-QFP-9	Bottom margin of porphyritic rhyolite member of the Doon Sill	NR 88482 29140
DD-QFP-10	Bottom margin of porphyritic rhyolite member of the Doon Sill	NR 88480 29180
DD-Dol-11	Xenocrystic basaltic andesite from base of the Doon Sill	NR 88480 29180
DD-Dol-11a	Xenocrystic basaltic andesite near internal margin with dacite, eastern side of Drumadoon Point Sill	NR 88278 28803
DD-Dol-12	Xenocrystic basaltic andesite near internal margin with dacite, eastern side of Drumadoon Point Sill	NR 88278 28803
DD-Dol-13	Xenocrystic basaltic andesite near internal margin with dacite, eastern side of Drumadoon Point Sill	NR 88278 28803
DD-QFP-15	Porphyritic rhyolite from Drumadoon Dyke	NR 88485 28715
DD-mDol-16	Aphyric basalt at margin of An Cumhann Dyke	NR 88392 31155
DD-mDol-17	Aphyric basalt (chemically andesite) from margin of An Cumhann Dyke; 10 cm from SE contact	NR 88392 31155
DD-mDol-18	Dacite near margin of An Cumhann Dyke; appeared to be xenocrystic basalt in the field; 30 cm from SE contact	NR 88392 31155
DD-QFP-19	Pale rhyolite, 6 m SE of NW margin of An Cumhann Dyke	NR 88421 31217
DD-QFP-21	Pale rhyolite, 6 m SE of NW margin of An Cumhann Dyke	NR 88421 31217
DD-Kspar	Single euhedral potassium feldspar crystals from quarry, SE corner of the Doon Sill	NR 88625 29145

isotopic data for the local crust were used where available (crustal data fields are from this study and Dickin *et al.*, 1981; Dickin & Bowes, 1991; Halliday *et al.*, 1993; Dickin, 1994) and further crustal samples ($n = 8$; see Table 4, below) were analysed to bridge any gaps in the dataset.

Sample preparation

Samples were sliced and weathered edges were removed. Samples were then crushed in a jaw-crusher to millimetre-sized pieces. Xenocrysts were excluded from the basaltic andesite by preferentially picking the matrix and were not analysed. Mafic enclaves were also excluded from the enclave-bearing rhyolite. The samples were then powdered in a tungsten carbide TEMA mill.

ANALYTICAL METHODS

X-ray fluorescence

Major and trace elements on all samples were determined by XRF at the GEOMAR Research Centre, Kiel, Germany. Samples were analysed on fused beads using a Philips PW1480 spectrometer. Analyses were performed with an Rh tube; calibration was performed using international geological reference samples (see Abratis *et al.*, 2002). Water and CO_2 were analyzed using an IR photometer (Rosemount CSA 5003). Major element data were normalized to 100% (volatile free) for plotting and subsequent modelling.

Inductively coupled plasma mass spectrometry

Rare earth element (REE) concentrations for the Drumadoon Intrusive Complex were determined by inductively coupled plasma mass spectrometry (ICP-MS) using a Hewlett Packard 4500 at the Institute F.-A. Forel, Versoix, Switzerland. Rare earth element concentrations for the Northern Granite and crustal samples were determined by ICP-MS at the Scottish Universities Environmental Research Centre (SUERC), East Kilbride, Scotland, using a VG Elemental PQ2 plus ICP-MS system fitted with a Meinhard nebulizer and a water-cooled glass Scott double-pass spray chamber. Further details on the instrument settings and procedures have been given by Olive *et al.* (2001). Analyses of geological reference standard BCR-1 ($n = 36$) yielded an average standard deviation of 0·38 ppm over mean values of 14 rare earth elements when compared with published values for BCR-1 (Raczek *et al.*, 2001).

Sr and Nd isotope ratios for the Drumadoon Intrusive Complex

Both strontium and neodymium isotope ratios for the samples from the Drumadoon Intrusive Complex were analysed at the Department of Mineralogy, University of Geneva, Switzerland.

Strontium isotopes

Sr was isolated using the method of Deniel & Pin (2001). Sr isotope ratios were measured by thermal ionization mass spectrometry (TIMS) using a seven-collector Finnigan MAT 262 system with extended geometry and stigmatic focusing using double Re filaments. The $^{87}Sr/^{86}Sr$ ratios were measured in semi-dynamic mode and were mass fractionation corrected to a $^{88}Sr/^{86}Sr$ ratio of 8·375209, and normalized to the $^{87}Sr/^{86}Sr$ ratio of 0·708000 for the Eimer & Amend $SrCO_3$ standard (Faure, 2001). Measured values of this standard during the period of this study were 0·708019 ± 54 (2σ, $n = 82$).

Neodymium isotopes

Nd separation was undertaken on a REE fraction from the Sr columns. It employed Eichrom TRU-Spec Resin (50–100 μm) in disposable PP columns in series with Ln-Spec Resin (50–100 μm), using the methods described by Pin & Santos Zaldegui (1997). Neodymium isotope ratios were measured by TIMS on a seven-collector Finnigan MAT 262 system with extended geometry and stigmatic focusing, using double Re filaments. $^{143}Nd/^{144}Nd$ was measured in semi-dynamic mode (quadruple collectors, measurement jumping mode), mass fractionation corrected to $^{146}Nd/^{144}Nd = 0·721903$, and normalized to the internal value for the La Jolla standard (0·511837). The mean of 101 replicated analyses of this standard during the period of this study was 0·511837 ± 20 (2σ).

Sr and Nd isotope ratios for Arran crustal samples

All crustal country rock samples from Arran were analysed for strontium and neodymium isotope ratios at the Scottish Universities Environmental Research Centre.

Strontium isotopes

Sr was separated using standard cation exchange techniques with a single pass through Bio-Rad AG50W-X-12 resin. Samples were loaded on single Ta filaments with 1M phosphoric acid. Isotope ratios were measured by TIMS on a VG Sector 54-30 system in dynamic multi-collection mode and corrected for instrumental mass fractionation using an exponential law and $^{87}Sr/^{88}Sr = 0·1194$. Total procedure blanks are <300 pg. The internal laboratory Sr Standard (NBS987) was analysed at 0·710254 ± 18 (2σ) for the duration of this study.

Neodymium isotopes

A REE fraction was collected by cation exchange from the same samples as the Sr fraction. Nd was then separated using standard anion exchange chemistry and analysed by TIMS using a VG Sector 54-30 system. The internal laboratory Nd Standard (J&M) was analysed at 0·511504 ± 9 (2σ) for the duration of this study.

^{40}Ar–^{39}Ar geochronology

Two large (5 mm), blocky, euhedral K-feldspar phenocrysts from the porphyritic rhyolite (from sample DD-Kspar) were loosely crushed using a pestle and mortar and a sieved fraction of 250–500 μm was picked under a binocular microscope for ^{40}Ar–^{39}Ar dating. One sample (DD-U) was leached in a mild HF (5%) solution at room temperature for 10 min. Both samples were washed several times in deionized water in an ultrasonic bath. They were analysed at the ^{40}Ar–^{39}Ar geochronology laboratory at the University of Lund, Sweden, using a Micromass 5400 mass spectrometer with a Faraday detector and an electron multiplier, a metal extraction line, containing two SAES C50-ST101 Zr–Al getters and a cold finger cooled to *c.* −155°C by a Polycold P100 cryogenic refrigeration unit. The samples were step-heated using a defocused 50 W CO_2 laser rastered over the samples to provide even heating. Samples were measured on the electron multiplier and time zero regressions were fitted to data collected from 10 scans over the mass range of 40–36. Peak heights and backgrounds were corrected for mass discrimination, isotopic decay and interfering nucleogenic Ca-, K-, and Cl-derived isotopes. ^{40}Ar blanks were calculated before every new sample and after every three unknown steps. ^{40}Ar blanks were between 4×10^{-16} and 2×10^{-16} moles. Blank values for masses 39–36 were all less than 7×10^{-18} moles. Blank values were subtracted for all incremental steps from the sample signal. Further details on analytical procedures have been given by Chew *et al.* (2008).

MAJOR ELEMENT GEOCHEMISTRY

Major element compositions for analysed samples from the Drumadoon Igneous Complex are listed in Table 2. A plot of total alkalis vs silica (TAS) (Fig. 7a) indicates the wide range of compositions present. The most primitive samples analysed are basaltic andesites, ranging to rhyolite with nearly 80% SiO_2. Volumetrically, however, the suite is distinctly bimodal, with only small volumes of intermediate (andesite or dacite) rock types. This represents a typical British and Irish Palaeogene Igneous Province Bunsen–Daly gap (Bunsen, 1851; Daly, 1925; Yoder, 1973; Dickin *et al.*, 1984).

Harker plots (Fig. 7b–g) of major elements vs silica all show distinctly linear trends, rather than the typical

Table 2: Major and trace element data for samples from the Drumadoon Intrusive Complex

Sample:	DD-QFP-1	DD-QFP-2	DD-QFP-3	DD-dQFP-4	DD-dQFP-5	DD-Dol-6	DD-Dol-7	DD-Dol-8	DD-QFP-9	DD-QFP-10
SiO_2	62·69	68·37	67·06	65·28	66·22	44·93	53·12	53·97	68·35	67·39
TiO_2	0·52	0·35	0·41	0·44	0·45	0·75	0·90	0·80	0·38	0·39
Al_2O_3	13·64	12·29	12·86	13·25	13·09	14·84	15·57	14·81	12·32	12·42
Fe_2O_3	5·81	3·90	5·25	4·95	4·72	9·82	9·68	9·78	4·90	6·06
MnO	0·11	0·10	0·13	0·11	0·11	0·18	0·15	0·20	0·08	0·13
MgO	2·81	1·33	2·06	2·24	2·87	4·25	6·57	6·41	2·98	3·26
CaO	3·87	3·34	2·70	3·60	2·18	11·46	8·18	8·26	1·65	1·60
Na_2O	2·73	2·75	2·94	2·60	2·04	2·39	2·54	2·41	2·54	2·47
K_2O	3·08	4·25	3·96	4·04	4·72	2·27	1·37	1·29	4·56	4·49
P_2O_5	0·05	0·05	0·05	0·06	0·06	0·07	0·08	0·07	0·05	0·05
H_2O	3·01	1·72	2·00	1·80	2·68	3·61	2·36	2·43	1·98	2·41
CO_2	1·95	1·79	1·13	1·89	1·22	5·96	0·81	0·65	0·83	0·78
Total	100·27	100·24	100·55	100·26	100·36	100·53	101·33	101·08	100·62	101·45
Co	43	39	41	27	18	48	57	52	37	30
Cr	47	23	32	40	38	87	111	113	37	37
Ni	29	2	13	17	19	76	89	90	12	13
V	98	42	65	79	81	181	222	209	59	71
Zn	64	61	57	57	61	57	86	75	55	51
Ce	108	142	120	146	108	74	39	45	117	101
La	120	69	63	65	57	34	—	56	43	110
Nb	16	22	20	18	22	11	7	8	19	17
Ga	20	16	14	18	19	18	15	15	17	15
Pb	18	19	22	22	24	21	10	12	17	21
Pr	18	12	13	13	12	5	—	9	9	22
Rb	73	106	101	82	99	44	34	29	98	98
Ba	761	877	857	943	896	485	313	373	911	885
Sr	95	84	88	94	57	137	145	141	64	63
Th	16	14	17	10	17	11	6	11	14	20
Y	57	53	53	49	58	36	36	34	48	49
Zr	188	231	206	197	206	140	118	106	188	192

Sample:	DD-Dol-11	DD-Dol-11a	DD-Dol-12	DD-Dol-13	DD-QFP-15	DD-mDol-16	DD-mDol-17	DD-mDol-18	DD-QFP-19	DD-QFP-21
SiO_2	53·83	53·42	51·77	54·05	71·01	45·02	55·80	60·50	77·01	76·50
TiO_2	0·81	0·79	0·79	0·79	0·26	0·76	0·69	0·50	0·15	0·17
Al_2O_3	15·02	14·78	15·06	14·84	12·92	15·01	14·02	12·92	11·16	11·40
Fe_2O_3	9·57	9·40	9·35	9·64	3·18	9·96	8·50	6·61	1·83	2·14
MnO	0·20	0·14	0·13	0·14	0·05	0·19	0·16	0·14	0·03	0·06
MgO	6·26	5·84	5·57	5·62	1·51	4·35	5·10	2·58	0·51	0·44
CaO	8·60	8·16	7·79	7·72	0·63	11·61	6·08	4·08	0·54	0·57
Na_2O	2·45	2·53	2·65	2·60	1·91	2·34	2·56	2·84	2·21	2·36
K_2O	1·29	1·43	1·44	1·67	6·68	2·27	2·16	3·53	4·82	4·87
P_2O_5	0·08	0·08	0·08	0·07	0·04	0·07	0·06	0·05	0·03	0·03
H_2O	2·35	1·49	1·52	1·23	1·82	3·01	1·97	1·48	1·13	1·13
CO_2	0·85	2·36	5·01	2·20	0·41	6·04	2·92	4·72	0·26	0·26
Total	101·31	100·42	101·16	100·57	100·42	100·63	100·02	99·95	99·68	99·93
Co	53	49	63	45	38	40	49	33	44	33
Cr	109	106	102	101	—	78	83	55	—	—
Ni	88	78	82	74	—	74	59	29	—	—
V	201	190	186	195	20	182	171	100	—	—
Zn	78	78	65	85	42	59	68	57	34	47
Ce	63	55	50	52	138	66	55	92	166	117
La	109	—	20	—	59	94	135	31	409	652
Nb	9	7	9	9	21	12	10	16	24	23
Ga	19	16	18	16	18	18	16	14	16	17
Pb	15	13	7	17	21	13	20	18	22	25
Pr	16	—	—	—	13	15	21	6	69	104
Rb	32	26	29	37	134	44	45	69	145	145
Ba	343	415	393	410	1193	452	441	673	648	649
Sr	146	160	190	152	53	135	132	104	39	34
Th	—	6	13	—	20	8	12	13	14	21
Y	33	35	33	37	67	38	39	51	73	67
Zr	109	111	109	119	222	145	124	164	166	183

Major element values are in weight per cent oxide, trace element values are in ppm. —, below detection limit. CO_2 and H_2O were measured independently using an IR photometer.

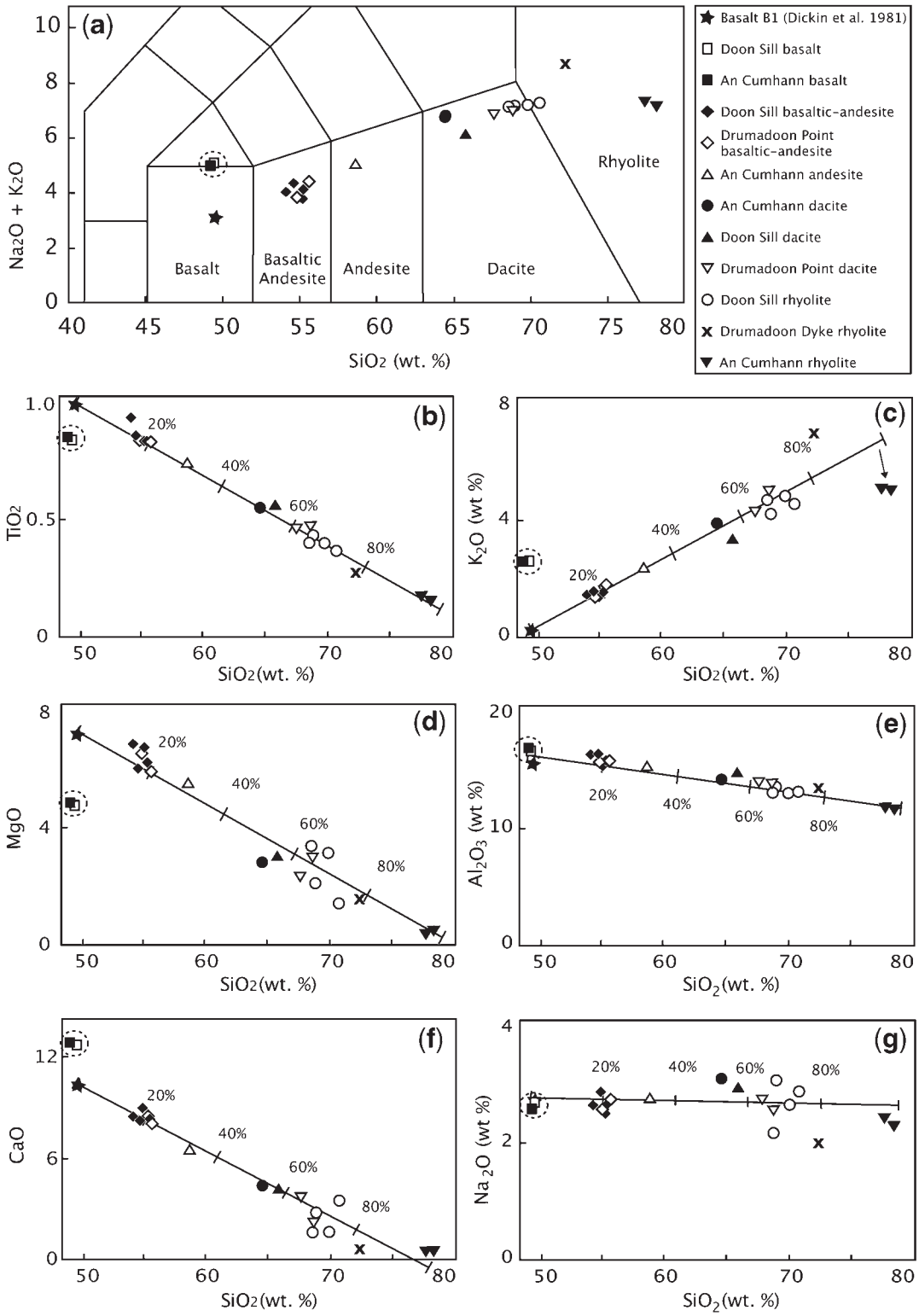

Fig. 7. (a) Total alkalis vs silica diagram showing the classification of the Drumadoon rock suite. The suite is sub-alkaline, with the majority of the samples classified as basaltic andesite, dacite and rhyolite. Small volumes of andesite and low-silica dacite bridge the Bunsen–Daly gap. Basalt Bl represents a 'normal' Arran basalt, containing no xenocrysts or evidence of mixing (Dickin *et al.*, 198l). (b) TiO_2 vs SiO_2. (c) K_2O vs SiO_2 showing binary mixing line. The distinct drop in K_2O at high SiO_2 concentrations should be noted; this is indicative of potassium feldspar fractionation. (d) MgO vs SiO_2; (e) Al_2O_3 vs SiO_2; (f) CaO vs SiO_2; (g) Na_2O vs SiO_2. Key for (b–g) as in (a). Basalt Bl was used as the basaltic end-member (the most mafic composition inferred at Drumadoon) as the basaltic andesites show clear evidence of mixing (presence of xenocrysts). All diagrams show a binary mixing line. Samples DD-dol-6 and DD-mDol-l6 plot off the main trend in almost all plots, indicating alteration of these marginal samples (dashed circle).

kinked trends that would result from the fractional crystallization of basaltic andesite to form rhyolite (see Geldmacher *et al.*, 1998). This suggests that the range of compositions may be the result of binary mixing, whereby two genetically unrelated end-members have mixed to form a range of intermediate magma compositions. This is particularly clear for MgO and TiO_2, which are normally depleted early as a result of the crystallization of olivine and Fe–Ti oxides (Fig. 7b and d). Na_2O shows the greatest scatter, probably caused by varying alkali feldspar phenocryst concentrations (Fig. 7g).

TRACE ELEMENT GEOCHEMISTRY

Trace element compositions are given in Table 2. When plotted versus SiO_2, variations in Sr, Ba, Zr, Cr and V show similar linear trends to the major elements (Fig. 8). This once again suggests that binary mixing rather than crystal fractionation was the principal process at work.

The alkali feldspar-compatible elements (e.g. Ba) show a significant downturn in the most evolved samples (the An Cumhann rhyolites) (Fig. 8b). This, together with a similar downturn in K_2O (Fig. 7c), indicates the continued crystallization of potassium feldspar in the magma reservoir after mixing had occurred. Zirconium also shows a significant downturn at high silica values, indicating post-mixing crystallization and fractionation of zircon (Fig. 8c).

Rare earth element patterns of the least and most evolved Drumadoon samples [basaltic andesite DD-Dol-12 (Drumadoon Point Sill) and rhyolite DD-QFP-19 (An Cumhann)] along with the patterns for the Northern Granite are illustrated in Fig. 8f and the data are reported in Table 3. The Northern Granite has previously been suggested to belong to the same phase of magmatism as the porphyritic rhyolites observed at Drumadoon (Kanaris-Sotiriou & Gibb, 1985). The Drumadoon REE patterns are relatively enriched in light REE (LREE). They are significantly enriched in LREE compared with the coarse-grained facies of the Northern Granite, and moderately depleted in heavy REE (HREE). This may be due to fractionation of LREE into residual liquids from the Northern Granite (see discussion below).

SAMPLES DD-DOL-6 AND DD-MDOL-16

Two basaltic samples, DD-Dol-6 (Doon) and DD-mDol-16 (An Cumhann) lie off the main trends in Figs 7 and 8. These samples were taken from the edges of the intrusions, in contact with the country rocks. They show high total volatile ($H_2O + CO_2$) contents of 9·57% and 9·05%, which is very high for igneous rocks, indicating that they contain a high proportion of hydrous alteration products. Unusually, however, these samples contain a very high proportion of CO_2 (5·96% and 6·04%) and DD-Dol-6 contains a large amount of interstitial calcite, as well as crosscutting calcite veins. These high volatile contents are surpassed only by the volatile contents of the local Triassic sandstone country rocks (Tables 4 and 5). These country rock sandstones have high total volatiles, at 10·68% (9·99% CO_2) for unbaked sandstones from ~30 m below the Doon Sill (sample A-TS) and 10·27% (7·93% CO_2) for baked sandstones and mudstones at the base of the sill (sample A-BTS). Locally, these sandstones are likely to have lost CO_2-rich fluids by devolatilization (decarbonation) reactions as a result of heating on intrusion of the complex (see Nabelek, 2007). These CO_2 fluids appear to have leached elements such as Ti (Fig. 7b), Cr and V (Fig. 8d and e) from the margins of the sill, as well as enriching other elements including K (Fig. 7c), Ba (Fig. 8b), Zr (Fig. 8c), Rb and Y. Although Ti, Y and Zr are not normally considered fluid mobile (Pearce & Cann, 1973), work by Hynes (1980) has shown these elements to be highly mobile in CO_2-rich fluids. Sample DD-mDol-16 is intruded into Permian sandstones, which do not have such high loss on ignition (LOI) values (see Table 5) but are very porous and permeable. CO_2-rich fluids released from the nearby Triassic rocks could have migrated through them and ponded at the sill–country rock interface.

CALCULATION OF THE INITIAL COMPOSITION OF THE MAFIC END-MEMBER

Based on phenocryst–xenocryst distribution densities, it is possible to estimate the approximate minimum volume of porphyritic rhyolite that would be required to mix with a mafic end-member to make a typical Drumadoon xenocrystic basaltic andesite. This technique can be used with any mixing pair where a known phenocryst phase is present in one end-member but not the other, and hence appears as identifiable xenocrysts within the mixed product. It relies on the assumption that no phenocrysts have been completely resorbed and there has been no segregation of melt and phenocrysts during mixing. The example below assumes that all the alkali feldspar xenocrysts in the basaltic andesite must have come from the rhyolitic end-member. By estimating the proportion of phenocrysts in a typical rhyolite, the minimum volume of rhyolite involved in mixing can be calculated using xenocryst density in the basaltic andesite product (see Takeuchi & Nakamura, 2001).

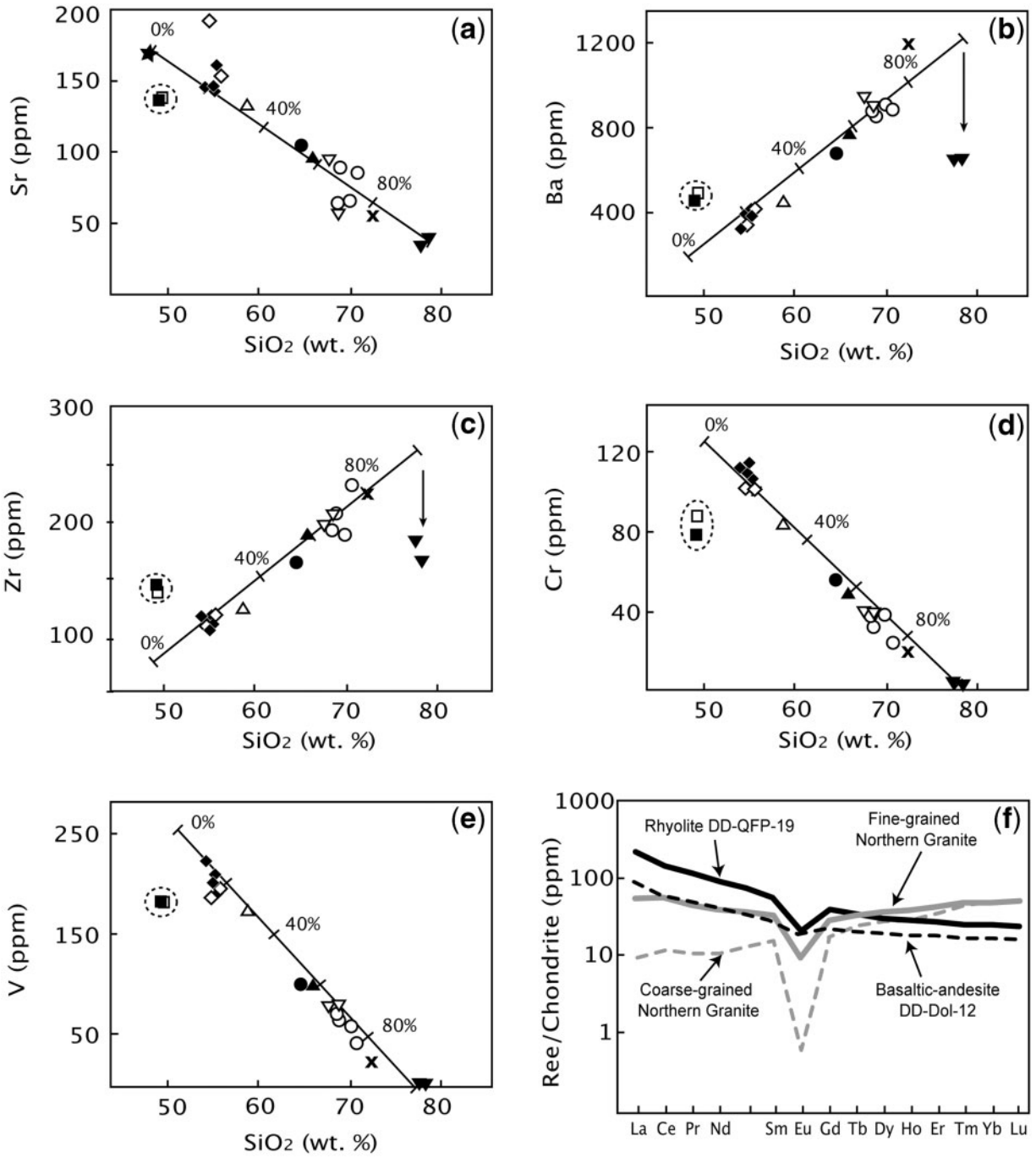

Fig. 8. (a) Variation of Sr vs SiO_2, consistent with a binary mixing line. More scatter is seen than in other element plots, probably as a result of variations in phenocryst concentration and xenocryst resorption. (b) Ba vs SiO_2. The distinct downturn in barium concentration at high contents of SiO_2 is in agreement with Fig. 7c, which shows a decrease in K_2O, suggestive of fractionation of potassium feldspar. (c) Zr vs SiO_2. The drop in Zr concentration may be due to late-stage zircon fractionation. Fractionation must have occurred post-mixing, but prior to emplacement, as minerals crystallized within the sill could not easily be removed from the melt to produce these depletion trends. Flow-induced liquid–crystal separation during intrusion may also have had an effect, separating feldspar and zircon crystals from the rhyolitic magma. (d) and (e) Cr and V vs SiO_2. These elements support binary mixing. Samples DD-dol-6 and DD-mDol-l6 show strong depletion in these transition metals. (f) Chondrite-normalized rare earth element patterns. Continuous black curve, rhyolite; dashed black curve, basaltic andesite; continuous grey curve, fine-grained Northern Granite; dashed grey curve, coarse-grained Northern Granite. It should be noted that the granites show enrichment in HREE, whereas the sill samples are enriched in LREE. Key as in Fig. 7a.

Table 3: Rare earth element compositions of the least (DD-Dol-12) and most (DD-QFP-19) evolved samples from the Drumadoon Intrusive Complex and the Northern Granite (ANG-1 and -2; coarse-grained and fine-grained facies)

Sample:	DD-Dol-12	DD-QFP-19	ANG-1	ANG-2
Rock type:	Basaltic andesite	Rhyolite	Coarse-grained granite	Fine-grained granite
La	21·47	30·74	3·01	15·09
Ce	39·85	57·26	9·92	37·31
Pr	4·81	6·84	1·34	4·66
Nd	19·56	26·61	6·63	19·54
Sm	4·46	5·73	3·17	5·74
Eu	1·06	1·05	0·04	0·65
Gd	4·91	5·99	4·50	7·24
Tb	0·84	0·99	1·12	1·56
Dy	5·39	6·41	9·23	11·85
Ho	1·13	1·32	2·26	2·73
Er	3·36	3·97	8·20	9·32
Tm	0·48	0·58	1·58	1·65
Yb	3·22	3·76	10·86	10·96
Lu	0·49	0·57	1·75	1·68

Granite samples are from North Glen Sannox, NE Arran. Values in ppm.

Table 4: Sample locations and lithologies for Midland Valley Terrane crustal samples

Sample number	Lithology and locality	Grid reference
MV-Ord	Ordovician greywacke, south of Girvan, South Ayrshire	NX 15285 93585
MV-Sil	Silurian sandstone, north of Muirkirk, East Ayrshire	NS 65667 36687
MV-Dev-WK	Devonian sandstone, West Kilbride, North Ayrshire	NS 21148 45321
MV-Carb-T	Carboniferous sandstone, Troon, South Ayrshire	NS 31613 30632
MV-Carb-SC	Carboniferous sandstone, Saltcoats, North Ayrshire	NS 24294 41041
A-Ps	Permian sandstone, Tormore Shore, Isle of Arran	NR 889 325
A-Ts	Triassic sandstone from shore below the Doon Sill	NR 88590 29644
A-BTs	Baked Triassic sandstone near path at base of the Doon Sill	NR 88658 29471

The proportion of the 'missing' end-member can then be approximated using the equation

$$M_x = \left(\frac{C_x}{C_p}\right)M_p + \left(1 - \frac{C_x}{C_p}\right)M_a$$

whereby the quantity of porphyritic (rhyolite) magma (M_p) that is mixed with the aphyric (basalt) magma (M_a) to make the xenocrystic (basaltic andesite) magma (M_x) is represented by the ratio of xenocrysts (C_x) (per area or volume) in the mixed magma to phenocrysts (C_p) (per area or volume) in the parental porphyry.

To calculate the proportion of the aphyric basalt magma, M_a, this equation can be rearranged to

$$M_a = \frac{M_x - \left[M_p\left(\frac{C_x}{C_p}\right)\right]}{\left(1 - \frac{C_x}{C_p}\right)}.$$

M_x and M_p can be replaced by either major element (wt %) or trace element (ppm) values to calculate the geochemical properties of the aphyric magma (M_a).

Relative proportions for these intrusions were estimated by analysing photographs of a typical rhyolite from Cleiteadh nan Sgarbh and comparing phenocryst

Table 5: Major and trace element data for Permian and Triassic sandstone samples

Sample:	A-Ps	A-Ts	A-BTs
Rock type:	Sandstone	Sandstone	Sandstone
SiO_2	86·33	66·98	53·98
TiO_2	0·18	0·27	0·64
Al_2O_3	6·59	5·05	12·25
Fe_2O_3	0·76	1·34	5·95
MnO	0·00	0·12	0·12
MgO	0·23	4·86	5·03
CaO	0·08	7·21	6·51
Na_2O	0·61	0·34	0·75
K_2O	3·90	2·64	4·57
P_2O_5	0·03	0·04	0·14
H_2O	0·52	0·69	2·34
CO_2	0·05	9·99	7·93
Total	99·28	99·53	100·21
Co	32	31	24
Cr	<17	19	68
Ni	–	5	23
V	23	25	75
Zn	9	41	74
Ce	45	<8	75
La	111	25	36
Nb	8	18	19
Ga	9	<6	18
Pb	10	13	21
Pr	21	<4	7
Rb	73	50	115
Ba	637	424	530
Sr	85	90	148
Th	<3	8	13
Y	6	15	26
Zr	95	328	184

Major element values are in weight per cent, trace element values are in ppm.
– indicates concentrations were below detection limit

distribution densities with photographs of a Drumadoon xenocrystic basaltic andesite dyke. Phenocryst–xenocryst densities were similar for each lithology across all the intrusions. Sites that afforded large, flat, polished outcrops for analysis were chosen. An ~21% by volume addition of porphyritic rhyolite to a mafic end-member is required to make basaltic andesite with the observed phenocryst–xenocryst distribution densities (Table 6). Samples from closer to the basaltic andesite–dacite and dacite–rhyolite margins show a much stronger rhyolite influence. Whereas the boundary between the basaltic andesite and dacite is distinct, there is a concentration of xenocrysts in the basaltic andesite within 15 cm of the boundary. This may be due to the rhyolite skimming off basaltic andesite liquid at the interface to form dacite. This would therefore maintain a distinct unchilled margin while concentrating the xenocrysts along the boundary.

A 21% volume addition of the most evolved rhyolitic composition (~78% SiO_2) would significantly affect the composition of a mafic magma. These values can be inserted into the equations above, using $C_x/C_p = 0{\cdot}21$, $M_p = 78$ and $M_x = 54$, a typical SiO_2 value for the basaltic andesites. The mafic end-member, prior to mixing (M_a), should therefore be a basalt with ~48% SiO_2. Compositionally, this value is comparable with other, less-evolved, basaltic samples analysed from Arran; for example, samples B1 (Judd's dyke 1, 100 m north of An Cumhann, NR 884 314) and B8 (south Arran, NS 019 210) (47·92%, 46·79%) from Dickin *et al.* (1981). Similarly, the calculated values of MgO and Fe_2O_3 for this mafic end-member (7·4% and 11·4% respectively) correlate well with the published B1 and B8 values (7·17%, 8·05% for MgO and 11·56%, 11·4% for recalculated FeO and Fe_2O_3 to $Fe_2O_{3\text{Tot}}$) (Dickin *et al.*, 1981). Based on these comparisons, the composition of basalt B1 of Dickin *et al.* (1981) is considered representative of the mafic end-member in this suite of samples.

Table 6: Phenocryst and xenocryst concentrations recorded from outcrop photographs, including the percentage of rhyolite needed to make the xenocrystic basaltic andesite

	Maximum density observed (per 10 cm^2)	Minimum density observed (per 10 cm^2)	Average (per 10 cm^2)	% rhyolite needed
Xenocrystic basaltic andesite				
<15 cm from margin with dacite	25	16	21	57
>15 cm from margin with dacite	11	8	9	21
Porphyritic rhyolite	53	32	42	

LEAST-SQUARES MIXING ANALYSIS

Least-squares mixing analysis of both major and trace element data was used to compare the dacitic sample suite with a modelled mixed composition (see Bryan *et al.*, 1969). This method produces a best-fit mixing ratio for the data using the Bl basalt (Dickin *et al.*, 1981) and An Cumhann rhyolite, DD-QFP-19, as end-members. As we preferentially avoided analysing feldspar xenocrysts when measuring major elements by XRF, only the TiO_2, MgO, CaO, MnO and Fe_2O_3 values of the Bl basalt (as they are not alkali feldspar compatible) were used for least-squares mixing analysis, making Bl directly comparable with our basaltic andesite values. Using these major element values, least-squares mixing analysis suggests that a mixture of 75:25 basalt to rhyolite was required to form the basaltic andesite (DD-Dol-12, $r^2 = 0{\cdot}07$), which is very similar to our ratio of 79:21 based on xenocryst concentrations. The extra 4% rhyolite needed for the least-squares model most probably reflects xenocrysts that were entirely resorbed within the basaltic andesite hybrid and so were not accounted for in the phenocryst-based estimations.

Maximum and minimum mixing ratios for the formation of the dacitic magma [DD-mDol-18 (64·93% SiO_2) and DD-QFP-5 (69·78% SiO_2)] were calculated at 41:59 and 24:76, with a sum of r^2 values at 1·02 and 1·15 respectively. These calculations once again used the An Cumhann rhyolite (DD-QFP-19) and the Bl basalt as end-members.

GEOCHRONOLOGY

^{40}Ar–^{39}Ar step heating yielded two dates of 59·04 ± 0·13 Ma (leached) and 59·16 ± 0·17 Ma (unleached) for an alkali feldspar separate from the porphyritic rhyolite (Table 7). Both samples yield plateaux (with low analytical uncertainties) using the criteria of Dalrymple & Lamphere (1972), which specify the presence of at least three contiguous incremental heating steps with statistically indistinguishable ages that constitute >50% of the total ^{39}Ar released during the experiment (Fig. 9). The significance of these age data is discussed below.

STRONTIUM AND NEODYMIUM ISOTOPE GEOCHEMISTRY

The igneous rocks of the intrusive complex show strong variation in $^{87}Sr/^{86}Sr_{(i)}$, with ranges of 0·706200–0·707973 ± 63 (2σ), 0·709631–0·710481 ± 12 (2σ) and 0·710064–0·712243 ± 55 (2σ) for the basaltic andesite, dacite and porphyritic rhyolite samples respectively. These values are significantly displaced from typical mantle values towards those of the regional crust (Fig. 10).

Table 7: ^{40}Ar–^{39}Ar data from the Drumadoon Igneous Complex

Power (W) equivalent to T	Ca/K	$^{36}Ar/^{39}Ar$	$^{40*}Ar/^{39}Ar$	Mol $^{39}Ar \times 10^{-14}$	$\%^{39}Ar$ in step	Cumulative % ^{39}Ar	% rad. ^{40}Ar	Age (Ma)	± Age
DD-U K-feldspar, J = 0·0183 ± 0·000012									
2	0·020	0·0011	1·781	0·51	8·3	8·3	84·4	57·86	0·26
0	0·023	0·0015	1·821	2·4526	39·9	48·1	81	59·15	0·13
2·3	0·018	0·0017	1·817	0·5831	9·5	57·6	78·5	59·03	0·26
2·5	0·021	0·0011	1·826	1·5115	24·6	82·2	85·4	59·29	0·13
2·9	0·036	0·0006	1·818	0·9713	15·8	98	91·7	59·03	0·14
4	0·068	0·0004	1·874	0·1246	2	100	93·7	60·84	1·12
Integrated age								59·10	0·20
Plateau age					91·7			59·16	0·17
DD-T K-feldspar, J = 0·01835 ± 0·000012									
2	0·023	0·0003	1·813	0·874	12·7	12·7	95·2	58·87	0·12
2·1	0·021	0·0009	1·817	0·4909	7·2	19·9	87·5	59·01	0·16
2·2	0·023	0·0010	1·820	1·648	24	43·9	85·6	59·11	0·12
2·3	0·033	0·0012	1·820	0·6666	9·7	53·7	84·2	59·10	0·16
2·5	0·027	0·0007	1·818	1·3028	19	72·7	89·6	59·06	0·12
3·5	0·026	0·0007	1·819	1·875	27·3	100	90·1	59·08	0·10
Integrated age								59·21	0·18
Plateau age					100			59·04	0·13

Data are corrected for machine blank, correction factors and $^{37}Ar/^{36}Ar$ post-irradiation decay. Step 1 in sample DD-U was not used in the calculation of the plateau age.

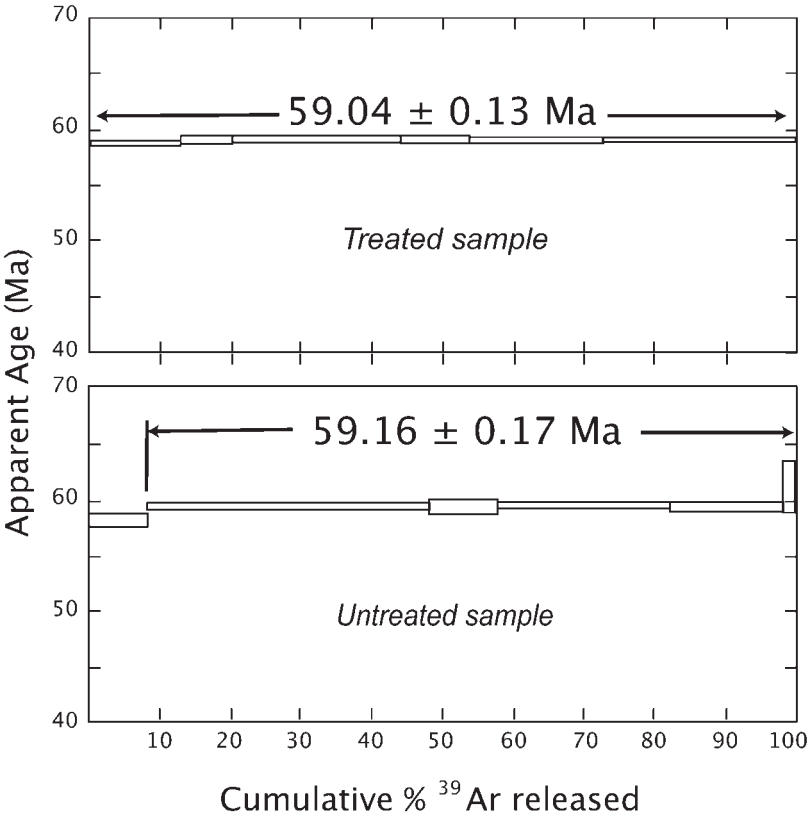

Fig. 9. ^{40}Ar–^{39}Ar plateaux diagrams for dated K-feldspar samples from the porphyritic rhyolite member of the Doon Sill. The upper sample (DD-T) has been treated in HF, whereas the lower sample (DD-U) is untreated.

Combined with the low Nd isotope ratios in some of the less evolved samples [0·512098 ± 8 (2σ) for DD-Dol-l3], these data provide strong evidence for crustal contamination (Tables 8 and 9).

The effects of late-stage magma mixing on isotope ratios

As described above, both the basaltic andesite and dacite appear to have mixed with significant volumes of rhyolite. Therefore, to better understand the initial isotopic composition of the two end-member magmas, samples must be 'un-mixed' to give their original isotope ratios, prior to magma mixing. This is important because the end-member magmas may not necessarily be genetically related and therefore may have had significantly different contamination histories. To do this, the proportion of basalt and rhyolite in each mixed sample was calculated from their major and trace element geochemistry (using the equations above). Using this proportion (x), the effect of magma mixing could be filtered out from the isotope data. The equation

$$M_m = x(B_i) + (1 - x)(R_i)$$

was used, whereby the mixed magma (M), is the sum of a certain fraction (x) of basalt (B) and the remainder ($1 - x$) of rhyolite (R). M_m is the isotope ratio of the mixed magma (known), B_i is the isotope ratio of the original basalt (unknown) and R_i is the isotope ratio of the most evolved rhyolite (DD-QFP-l9) (assumed to represent the rhyolitic end-member). This equation can be rearranged to two forms,

$$B_i = \frac{M_m - R_i + x(R_i)}{x}$$

where $x > 0{\cdot}5$, and

$$R_i = \frac{M_m - x(B_i)}{1 - x}$$

where $x < 0{\cdot}5$.

In the case of a magma that contains more basalt than rhyolite ($x > 0{\cdot}5$), the rhyolitic component was removed, yielding an estimate of the pre-mixing basaltic isotope ratio (B_i). The samples that contain more rhyolite than basalt ($x < 0{\cdot}5$) had the basaltic component removed. This step could only be estimated, as there is no pristine primitive basaltic end-member in the dataset. Instead, the recalculated initial isotopic compositions of the least-mixed basaltic andesite sample (DD-Dol-l1) were used (0·704816, 0·512329). This appears to be a suitable choice, as all the dacite samples corrected using this value produce similar

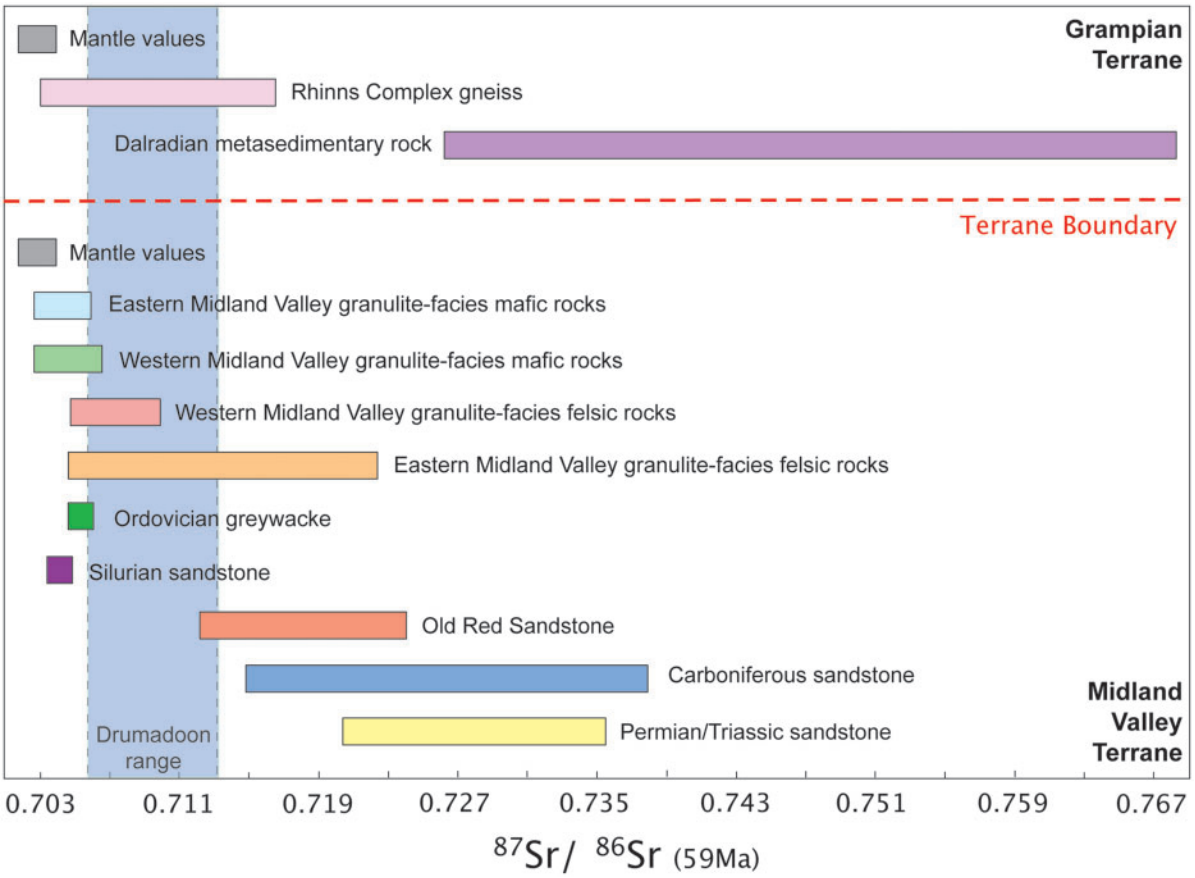

Fig. 10. Bar chart of strontium isotope ratios, showing the ranges of crustal values in the Arran region and the strontium isotope range of igneous samples from the Drumadoon Intrusive Complex (vertical shaded block). Samples are divided based on their crustal terrane affinity. The igneous rocks are displaced from mantle values towards crustal compositions. Crustal data fields are from this study, Dickin *et al.* (1981), Dickin & Bowes (1991), Halliday *et al.* (1993) and Dickin (1994).

Table 8: Measured and age-corrected strontium and neodymium ratios for samples from the Drumadoon Intrusive Complex

Sample no.	Rb (ppm)	Sr (ppm)	Sm (ppm)	Nd (ppm)	$^{87}Sr/^{86}Sr$ measured	2σ	$^{143}Nd/^{144}Nd$ measured	2σ	$^{87}Sr/^{86}Sr$ (59·16 Ma)	$^{143}Nd/^{144}Nd$ (59·16 Ma)
DD-QFP-1	73	95	9	44	0·711732	0·000007	0·512187	0·000003	0·709881	0·512140
DD-QFP-2	106	84	10	52	0·714061	0·000008	0·512173	0·000004	0·711074	0·512129
DD-QFP-3	101	88	9	49	0·712751	0·000012	0·512175	0·000005	0·710064	0·512130
DD-dQFP-4	82	94	9	45	0·712669	0·000007	0·512174	0·000005	0·710481	0·512129
DD-dQFP-5	99	57	9	47	0·714621	0·000010	0·512211	0·000004	0·710405	0·512165
DD-Dol-6	44	137	5	25	0·708636	0·000010	0·512264	0·000005	0·707896	0·512213
DD-Dol-8	29	141	4	19	0·706686	0·000008	0·512326	0·000004	0·706200	0·512273
DD-QFP-9	98	64	9	47	0·714698	0·000007	0·512184	0·000004	0·710853	0·512140
DD-QFP-10	98	63	9	45	0·714535	0·000007	0·512170	0·000004	0·710765	0·512125
DD-Dol-11	32	146	4	20	0·706811	0·000008	0·512336	0·000007	0·706329	0·512283
DD-Dol-11a	26	160	4	20	0·707048	0·000063	0·512321	0·000005	0·706631	0·512268
DD-Dol-12	29	190	4	19	0·707962	0·000005	0·512308	0·000006	0·707641	0·512257
DD-Dol-13	37	152	5	23	0·707306	0·000005	0·512150	0·000008	0·706777	0·512098
DD-QFP-15	134	53	11	59	0·717721	0·000006	0·512172	0·000004	0·711884	0·512128
DD-mDol-16	44	135	5	25	0·708662	0·000007	0·512281	0·000004	0·707973	0·512231
DD-mDol-17	45	132	6	27	0·707860	0·000007	0·512245	0·000005	0·707074	0·512195
DD-mDol-18	69	104	8	38	0·711216	0·000009	0·512200	0·000005	0·709631	0·512152
DD-QFP-19	145	39	12	62	0·721596	0·000055	0·512155	0·000004	0·712021	0·512109
DD-QFP-21	145	34	10	51	0·721948	0·000008	0·512143	0·000005	0·712243	0·512095
DD-Kspar	109	204	1	3	0·714823	0·000009	0·512182	0·000007	0·713527	0·512141

Table 9: Measured and age-corrected strontium ratios for crustal samples from the Midland Valley Terrane

Sample	Rb (ppm)	Sr (ppm)	$^{87}Sr/^{86}Sr$ measured	2σ	$^{87}Sr/^{86}Sr$ (59·16 Ma)
MV-Ord	16	204	0·706087	0·000026	0·705896
MV-Sil	50	12	0·714753	0·000028	0·704614
MV-Dev-WK	41	152	0·720041	0·000042	0·719385
MV-Carb-T	25	45	0·716288	0·000034	0·714936
MV-Carb-SC	207	1648	0·735053	0·000030	0·734746
A-Ps	73	85	0·737474	0·000026	0·735380
A-Ts	50	90	0·733688	0·000026	0·732334
A-BTs	115	148	0·730253	0·000030	0·728359

isotopic values to sample DD-QFP-19, the rhyolitic end-member. These estimated B_i values are also very similar to Sr and Nd values published for other Arran basalts (Dickin *et al.*, 1981; Dickin, 1994), and yield isotope ratios that are likely to be representative of the local mafic magma prior to mixing. (See Table 10 for recalculated values.)

Modelling of crustal contamination

Considering the proximity of the Drumadoon Intrusive Complex to a major terrane boundary (Fig. 2), our data were compared with published data fields for crustal lithologies from both the Midland Valley and Grampian terranes (Figs 10–12) (Dickin *et al.*, 1981; Marcantonio *et al.*, 1988; Dickin & Bowes, 1991; Halliday *et al.*, 1993; Dickin, 1994), along with new data (this study) from Midland Valley Palaeozoic sediments collected from Arran and the Ayrshire region of southwestern Scotland. Using a typical Atlantic mid-ocean ridge basalt (MORB) composition (Saunders *et al.*, 1988) and the various crustal compositions as end-members, geochemical models for both assimilation during fractional crystallization (AFC) (DePaolo, 1981) and bulk isotope mixing (Langmuir *et al.*, 1978) were produced. MORB values were used as the mantle end-member, as there is significant evidence that the crust has influenced even the most primitive samples within the BIPIP (Palacz, 1985; Geldmacher *et al.*, 1998; Troll *et al.*, 2004, 2005) and a depleted mantle source has been envisaged for much of the BIPIP (Gamble *et al.*, 1992; Ellam & Stuart, 2000).

AFC modelling used the *AFC.isotopes* program of J. Entenmann (http://www.geologynet.com/afc.isotopes.zip), based on the equations of DePaolo (1981). Samples were modelled for both binary mixing and AFC, and the process that yielded the best fit to the data was chosen. AFC modelling was performed over a range of r values (the ratio of assimilation to fractional crystallization), to evaluate the effect of various amounts of assimilation (see Reiners *et al.*, 1995).

Geochemical modelling of contamination by Midland Valley Terrane crust

As the Drumadoon Intrusive Complex lies within the Midland Valley Terrane (MVT), those crustal lithologies were initially considered as a potential source of contamination.

The MVT lies between the Highland Boundary Fault and the Southern Uplands Fault (Figs 1 and 2). Structurally, it forms a graben, in which mostly Palaeozoic rocks are exposed. The Ordovician, Silurian and Devonian sequences comprise sandstones and mudstones. The Carboniferous sandstones in this region are deltaic sequences whereas the Permo-Triassic deposits, seen in the Arran area, are mostly aeolian and fluvial sandstones (Trewin, 2002).

The basement to the Midland Valley Terrane is known from xenolith suites entrained within Carboniferous volcanic rocks and comprises both mafic and felsic granulite-facies metamorphic rocks (Bamford *et al.*, 1977; Graham & Upton, 1978; Halliday *et al.*, 1993), along with rare granulite-facies xenoliths, which are inferred to represent relict metasedimentary rocks. Zircons from one of these relict metasedimentary xenoliths have yielded early Proterozoic (>2 Ga) bulk fraction U–Pb upper intercept ages, indicating the presence of old detritus in the sedimentary precursor (Halliday *et al.*, 1984). The MVT basement xenoliths are thought to represent the lower portions of the crust in the area, at depths of 20–30 km, and yield Sm–Nd model ages of 0·6–1·8 Ga (Halliday *et al.*, 1993). For the purpose of this study they were divided into four groups (using the data and groupings of Halliday *et al.*, 1993) (Fig. 1):

(1) mafic granulite-facies xenoliths from the western MVT (Ashentree Glen, Heads of Ayr, Baidland Hill, Hawk's Nib);
(2) felsic granulite-facies xenoliths from the western MVT (Dunaskin Glen, Holmbyre, Baidland Hill);
(3) mafic granulite-facies xenoliths from the eastern MVT (Fidra, Partan Craig);
(4) felsic granulite-facies xenoliths from the eastern MVT (Briggs of Fidra, Partan Craig, Coalyard Hill).

When modelled as potential crustal contaminent end-members, the granulite-facies xenoliths sampled from western Scotland (mafic and felsic) (Halliday *et al.*, 1993) are not sufficiently radiogenic to contribute significantly to the strongly radiogenic isotopic signature (both in strontium and neodymium) of the Drumadoon magmas (Fig. 10). Similarly, even the most radiogenic xenoliths from eastern Scotland could not produce the isotopic

Table 10: Strontium and neodymium isotope ratios for samples from the Drumadoon Intrusive Complex, with the effects of magma mixing removed

Sample name	Proportion of basalt in mixed magma x	Sr isotope ratio of mixed magma M_m	Sr isotope ratio of rhyolitic end-member R_i	Calculated initial Sr ratio of basaltic end-member B_i	Nd isotope ratio of mixed magma M_m	Nd isotope ratio of rhyolitic end-member R_i	Calculated initial Nd ratio of basaltic end-member B_i
	$x > 0{\cdot}5$						
DD-DoI-11	0·79	0·706329	0·712021	**0·704816**	0·512283	0·512109	**0·512329**
DD-DoI-8	0·77	0·706200	0·712021	0·704461	0·512273	0·512109	0·512321
DD-DoI-11a	0·76	0·706631	0·712021	0·704929	0·512268	0·512109	0·512319
DD-DoI-12	0·76	0·707641	0·712021	0·706257	0·512257	0·512109	0·512303
DD-DoI-13	0·75	0·706777	0·712021	0·705028	0·512098	0·512109	0·512095
DD-mDoI-17	0·62	0·707074	0·712021	0·704042	0·512195	0·512109	0·512247

Sample name	Proportion of basalt in mixed magma x	Sr isotope ratio of mixed magma M_m	Sr isotope ratio of basaltic end-member B_i	Calculated initial Sr ratio of rhyolitic end-member R_i	Nd isotope ratio of mixed magma M_m	Nd isotope ratio of basaltic end-member B_i	Calculated initial Nd ratio of rhyolitic end-member R_i
	$x < 0{\cdot}5$						
DD-mDoI-18	0·41	0·709631	0·704816	0·712977	0·512152	0·512329	0·512029
DD-QFP-1	0·37	0·709881	0·704816	0·712856	0·512140	0·512329	0·512029
DD-QFP-10	0·31	0·710765	0·704816	0·713438	0·512125	0·512329	0·512034
DD-dQFP-4	0·3	0·710481	0·704816	0·712908	0·512129	0·512329	0·512044
DD-QFP-3	0·28	0·710064	0·704816	0·712105	0·512130	0·512329	0·512053
DD-dQFP-5	0·28	0·710405	0·704816	0·712578	0·512165	0·512329	0·512102
DD-QFP-9	0·24	0·710853	0·704816	0·712759	0·512140	0·512329	0·512080
DD-QFP-2	0·22	0·711074	0·704816	0·712839	0·512129	0·512329	0·512073
DD-QFP-15	0·08	0·711884	0·704816	0·712499	0·512128	0·512329	0·512111
DD-QFP-21	0·01	0·712243	0·704816	0·712318	0·512095	0·512329	0·512093
DD-QFP-19	0	0·712021	0·704816	**0·712021**	0·512109	0·512329	**0·512109**

The table shows the values used for each term in the recalculation equation. The values in bold were used as end-members. The data used for M_m were age corrected to 59·16 Ma prior to the calculations being performed.

compositions observed in the Drumadoon Intrusive Complex without unrealistic levels of assimilation (Fig. 10). Modelled results show AFC of the eastern MVT felsic granulite (sample PC347, Halliday *et al.*, 1993) of up to 15% melt remaining would be needed to form the Drumadoon rhyolites (at $r = 0{\cdot}4$). Typically, the physical limit of AFC models at $r = 0{\cdot}4$ is ~50% melt remaining, considering an assimilant of granitic composition (Reiners *et al.*, 1995). Bulk mixing of up to 87% mafic granulite (sample FD287, Halliday *et al.*, 1993) would be needed to produce the radiogenic signature of the Drumadoon basaltic andesites (Fig. 11). This would equate to almost total melting of the granulite-facies crustal material. Therefore, from the available data for the MVT, which are admittedly sparse, it appears that its lower crustal basement was not significantly involved in the contamination of the Drumadoon magmas.

A similar situation occurs when the Late Palaeozoic lithologies of the Midland Valley Terrane upper crust are considered (Table 9). The Ordovician and Silurian greywackes are not sufficiently radiogenic to have contributed significantly to the $^{87}Sr/^{86}Sr$ values observed at Drumadoon (Fig. 10). When the Devonian sandstones were modelled, it was found that it would require assimilation during fractional crystallization to ~15–20% melt remaining to make the rhyolites, once again making them an unrealistic end-member contaminant. The Carboniferous sandstones, although sufficiently radiogenic, are not deemed voluminous enough in the region to have had a significant influence on the magmas.

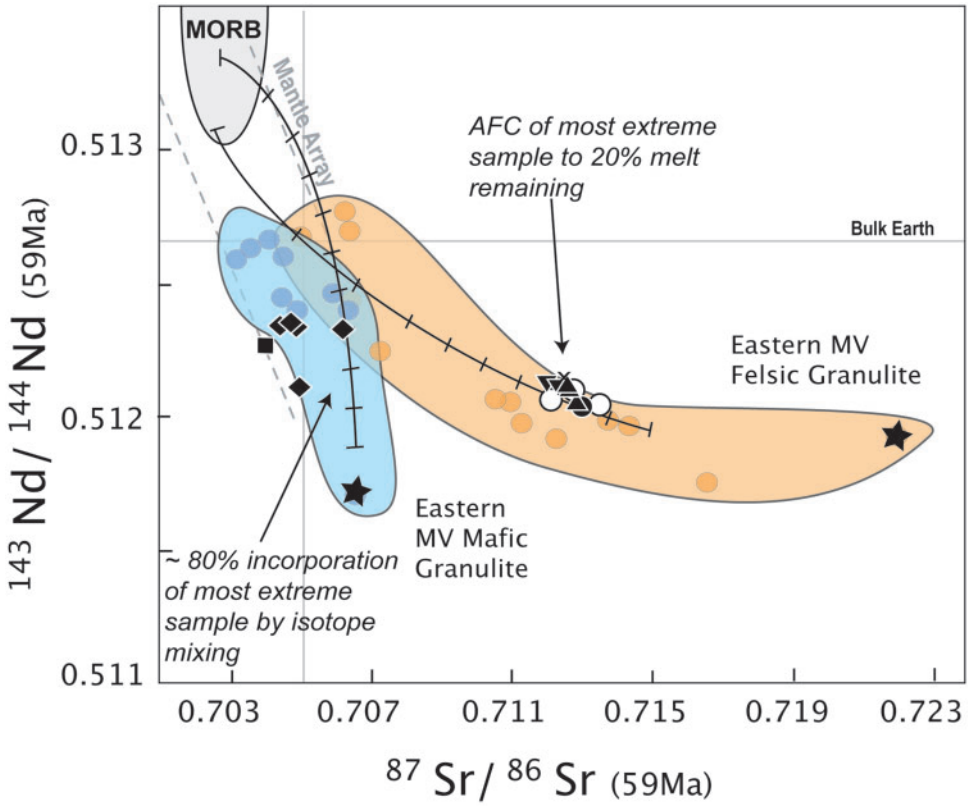

Fig. 11. The Nd–Sr isotope models for crustal contamination of the Drumadoon magmas, using the granulites of the Eastern Midland Valley. Crustal data fields from Halliday *et al.* (1993). The data have had the effects of magma mixing removed. Key as in Fig. 7a. Stars represent compositions used for geochemical modelling. Background grey circles represent the data points that make up each crustal field. Errors bars on the Drumadoon data are within the size of the symbols.

Only the country rock to the sills (the Triassic sandstone) shows any indication of having influenced the magmas. However, this influence is not apparent in the isotope composition of the igneous rocks, but rather in their major, trace and volatile element compositions.

Geochemical modelling of contamination by Grampian Terrane crust

Even though the Drumadoon Intrusive Complex lies within the Midland Valley Terrane, it appears that the majority of the crustal influence on the parental magmas must have resulted from interaction with Grampian Terrane lithologies. The Grampian Terrane is bounded by the Great Glen Fault to the north (Figs 1 and 2). The terrane is dominated by the Neoproterozoic–Cambrian (~800–520 Ma) rocks of the Dalradian Supergroup, a series of metasedimentary rocks initially deposited in an intra-cratonic basin that was to become the passive margin of Laurentia (Anderton, 1982). These sediments comprise sandstones, siltstones and mudstones, which were metamorphosed to greenschist–amphibolite-facies conditions during the 475–465 Ma Grampian Orogeny. This event represented the collision of an ophiolite–island arc terrane with the Laurentian margin as the Iapetus Ocean began to close (Dewey, 2005). The southern margin of the Grampian Terrane is marked by the Highland Boundary Fault (HBF) (Figs 1 and 2), which separates it from the Midland Valley Terrane. The present-day HBF is a steep, NW-dipping, post-Early Devonian reverse fault, which probably terminates as it reaches Arran (Tanner, 2008). Tanner (2008) did not attribute major tectonic significance to this structure, but it should be noted that there is evidence for a fundamental change in the nature of the basement at depth across this structure. The Highland Boundary Fault continues into western Ireland (see Chew, 2003), where it is clear that the Laurentian margin rocks are bounded to the SE by a Grampian island arc terrane. Unfortunately, apart from the studies of the xenolith suites reported above, the MVT basement south of the HBF in Scotland is not known.

The basement to the Dalradian sediments has not been directly observed in Scotland, but has been recognized both geophysically (Hall *et al.*, 1984) and geochemically (Frost & O'Nions, 1985; Dickin & Bowes, 1991; Hitchen

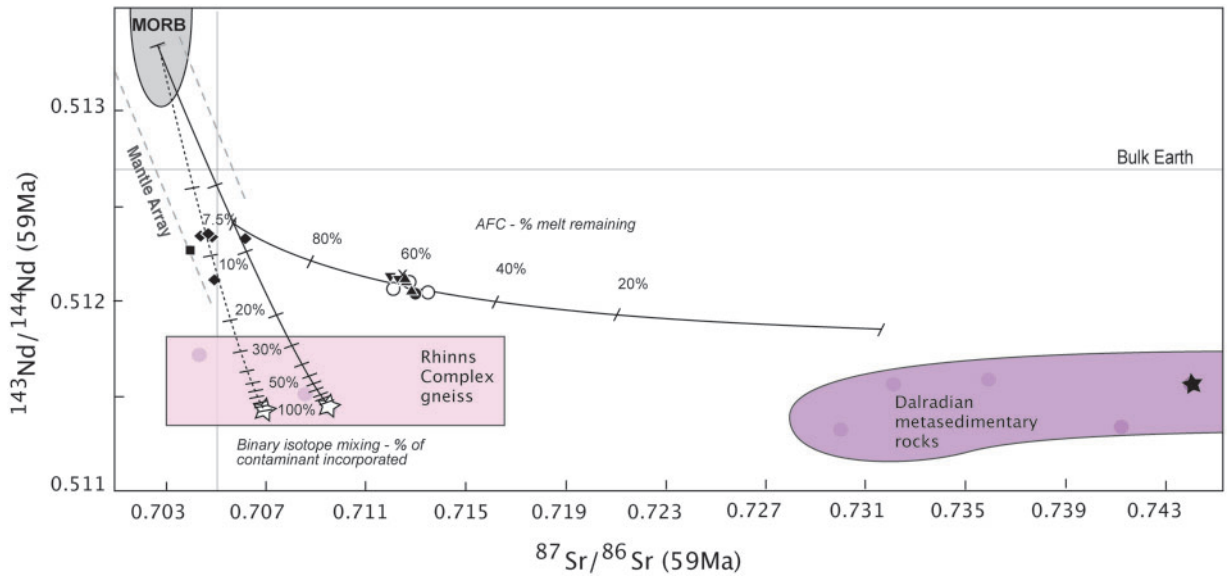

Fig. 12. Assimilation and fractional crystallization (AFC) and binary isotope mixing models of Grampian Terrane crustal contamination in the Drumadoon magma suite. Samples have had the effects of magma mixing removed to estimate initial pre-mixing isotope ratios. A partial melt of Dalradian metasediment (containing just a fusible mica component), would have a more radiogenic Sr isotope ratio and would plot to the right of the whole-rock values shown. Crustal data fields from Dickin *et al.* (1981), Marcantonio *et al.* (1988), Dickin & Bowes (1991) and Dickin (1994). Stars represent data points used for geochemical modelling. Errors bars on the Drumadoon data are within the size of the symbols.

et al., 1997; Dickin & Durant, 2002). In those studies it has been demonstrated that Late Caledonian (400 Ma) granites were influenced by a crustal component similar to a Rhinns Complex-type gneiss, and suggested that this may compose the underlying basement to the Grampian Terrane. Work by Daly *et al.* (1991) and Marcantonio *et al.* (1988) links Rhinns Complex gneisses on Islay with those on Inishtrahull in Northern Ireland, extending the region of known Proterozoic gneissic basement to the west. Together, these data suggest that the lower crust takes the form of a southward narrowing, wedge-shaped, parallel-sided block, of the order of 600 km east–west, and extending ~100 km north–south, obscured by the overlying Dalradian sequence (Dickin, 1992). Additionally, on the island of Colonsay, the Colonsay Group, a possible Dalradian Supergroup correlative, lies unconformably on Rhinns Complex gneisses (Fitches *et al.*, 1990).

Accordingly, Dalradian metapelite and Rhinns Complex gneiss (Marcantonio *et al.*, 1988) compositions were modelled as potential end-members. Incorporation of between 7 and 10% gneiss by bulk mixing could potentially produce the initial basalts at Drumadoon, with one sample yielding mixing values of up to ~13% gneiss (Fig. 12). The gneisses do not have enough radiogenic strontium to have been the sole influence on the rhyolitic magma. Similarly, the Dalradian metasediments require AFC to unrealistic levels if they were the sole contaminant forming the rhyolitic magma. However, a feasible mechanism for producing the rhyolites could involve a two-step contamination process, with initial mixing of 2–7·5% basement gneiss [sample PH2, Marcantonio *et al.* (1988); $^{87}Sr/^{86}Sr = 0{\cdot}71802 \pm 2$, $^{143}Nd/^{144}Nd = 0{\cdot}51150 \pm 2$] followed by assimilation of Dalradian upper crustal cover during fractional crystallization to ~55% melt remaining at $r = 0{\cdot}7$ (Fig. 12). Such high r values are reasonable considering the fertility of this kind of metasedimentary crust, with a large proportion of fusible, hydrous, K- (and hence Rb-) bearing phases such as biotite and muscovite (see Reiners *et al.*, 1995). Assimilation of a partial melt solely sourced from these fusible components would yield a more radiogenic contaminant than the whole-rock isotope ratio (see Duffield & Ruiz, 1998). If this was the case for assimilation of the Dalradian metasediments, values similar to those observed at the Drumadoon Intrusive Complex could be reached at higher proportions of remaining melt (i.e. AFC to >55% melt remaining).

DISCUSSION

Major and trace element data

Major and trace element data clearly show evidence of binary mixing between two end-member magmas, a porphyritic rhyolite and a basalt. Phenocryst–xenocryst and least-squares mixing analysis suggest mixing ratios of 79%:21% and 75%:25% respectively, to form the xenocrystic basaltic andesite, with the 4% difference probably representing phenocrysts that have been resorbed.

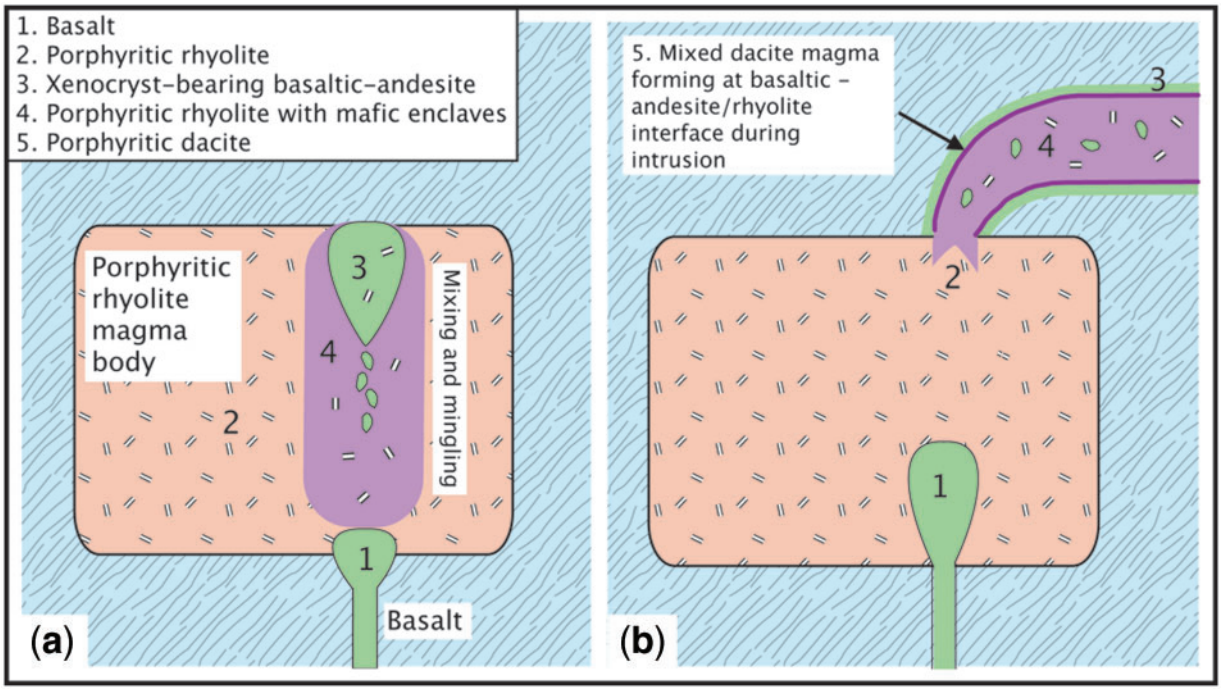

Fig. 13. Schematic diagram showing the intrusion sequence of the magmas at Drumadoon. (a) Basaltic magma (1) meets porphyritic rhyolite (2) in Grampian crust and mixes to form xenocrystic basaltic andesite (3). Mingling forms the enclave-bearing rhyolite (4). (b) Xenocrystic basaltic andesite (3) enters the conduit first, lubricating the way for enclave-bearing rhyolite (4), which forms the majority of the sill. The magmas interact in the conduit to form porphyritic dacite (5). Rhyolite with no mafic influence enters the conduit last (2) and is seen at the centre of the feeder dykes and at the top of the main sill.

The dacites were formed by mixing in the range of 41%:59% to 24%:76%.

The rhyolite samples exhibit evidence of post-magma mixing loss of potassium feldspar, as the mixing lines suggest that the rhyolitic end-member had much higher initial concentrations of potassium feldspar compatible elements (e.g. K_2O, Ba, Ce, Eu) (Figs 7 and 8). The downturn in these trends suggests that potassium feldspar has been lost from the rhyolitic magma, either by fractional crystallization or as the result of liquid–crystal separation during flow when the viscous porphyritic rhyolite was intruded. Physical mixing to form the basaltic andesite and enclave-bearing rhyolite must have occurred within the magma chamber, as post-intrusion (*in situ*) crystallization of feldspar from the rhyolitic magma would not have changed the bulk composition of the rhyolite samples. The presence of phenocrysts in the basaltic–andesite outside the marginal dacite-mixing front (which probably formed during intrusion) also suggests that the majority of mixing occurred within the magma chamber.

Based on these observations and inferences, an intrusion sequence can be envisaged (Fig. 13a and b) whereby a basaltic magma mixed with a porphyritic rhyolite magma to form the xenocrystic basaltic andesite and mingled to form the enclave-bearing rhyolite. The enclave-bearing rhyolite and basaltic andesite intruded together to form the composite intrusions. During intrusion, the dacitic magma formed at the interface between the basaltic andesite and rhyolite magmas in the conduit. Finally the rhyolite itself entered the conduit, forming the top of the main Drumadoon Sill and the centre of the An Cumhann feeder dyke.

Kanaris-Sotiriou & Gibb (1985) have previously suggested that the porphyritic rhyolites and the Northern Granite magmatic episodes may be related. Rare earth element patterns comparing the porphyritic rhyolite with the granite show that the granite is significantly depleted in LREE, with moderate HREE enrichment (Fig. 8). This does not discount a genetic relationship, as such depletion may be due to the fractionation of late-stage REE minerals from the granitic magma, some of which [e.g. fergusonite (a REE oxide) and gadolinite (a REE silicate)] have been observed in the Northern Granite (Hyslop *et al.*, 1999).

Significance of the age dates

The most recent ^{40}Ar–^{39}Ar date for the Northern Granite is for a biotite mineral separate dated by Chambers (2000) at $57{\cdot}85 \pm 0{\cdot}15$ Ma (weighted mean average). This does not overlap with our dates for the Drumadoon porphyritic

Table 11: Available radiometric and palaeomagnetic ages for the porphyritic rhyolite sills of Arran (and surrounding areas) and the Northern Granite

Study	Site dated	Method of dating	Date
This study	K-feldspar separate from Drumadoon Sill	^{40}Ar–^{39}Ar step heating	59·05 ± 0·13 Ma 59·16 ± 0·17 Ma plateau age
Mussett *et al*. (1987)	Whole-rock(?) from Drumadoon Dyke	^{40}Ar–^{39}Ar step heating	58·5 ± 0·8 Ma
Buist *et al*. (1979)	Bute composite sill	K–Ar dating	Minimum age of 56·3 ± 1·0 Ma
Chambers (2000); Emeleus & Bell (2005)	Northern Granite, biotite separate	^{40}Ar–^{39}Ar step heating	57·35 ± 0·22 Ma 58·64 ± 0·34 Ma 58·07 ± 0·25 Ma 57·85 ± 0·15 Ma (WMA)
Dickin *et al*. (1981)	Northern Granite, whole-rock	Rb–Sr isochron	60·3 ± 1·6 Ma
Evans *et al*. (1973)	Feldspar–quartz concentrate from Northern Granite	^{40}Ar–^{39}Ar age spectrum	58·8 ± 0·6 Ma; corrected to 60·3 ± 0·6 Ma by Hodgson *et al*. (1990)
Hodgson *et al*. (1990)	Northern Granite Drumadoon Sill Brown Head Sill Bennan Head Sill	Palaeomagnetic polarity	Northern Granite and porphyritic rhyolite sills suggested to have formed in same period of normal polarity, chron 26, from 58·7 to 58·4 ± 0·2Ma (Gradstein *et al*., 2004)
Mussett *et al*. (1989)	Dun Dubh plug Bute composite sill	Palaeomagnetic polarity	Normal polarity, attributed to same period of normal polarity as the other rhyolite intrusions
Mussett *et al*. (1987)	Judd 4 Dyke Cleiteadh Nan Sgarbh Dyke Drumadoon Sill Drumadoon Dyke Brown Head Sill Bennan Head Sill	Palaeomagnetic polarity	Activity on Arran spans a R–N–R period; all porphyritic rhyolites are normal. Attributed to ~58·5 Ma

WMA: weighted mean average

rhyolite (59·04 ± 0·13 Ma and 59·16 ± 0·17 Ma). This suggests that the chemical similarities mentioned above may be the result of temporally distinct batches of similar parental magma passing through and assimilating identical crustal lithologies, and that felsic magmatism on Arran had a protracted duration.

Previous palaeomagnetic work on both the quartz- and feldspar-phyric rhyolite suite and the Northern Granite has suggested that all the intrusions formed within the same period of normal polarity (chron 26n) (Mussett *et al*., 1987, 1989; Hodgson *et al*., 1990; Table 11). However, in light of the more precise radiometric dates from both this study and that of Chambers (2000), it seems that the Northern Granite may lie within chron 26n, whereas the Drumadoon Sill was intruded during a period of normal polarity within chron 26r (Fig. 14). These data provide further evidence for normal polarity subchrons within chron 26r, as inferred on the Isle of Mull, Scotland, by Chambers & Pringle (2001). The work of Hodgson *et al*. (1990) had previously suggested a magnetostratigraphy of

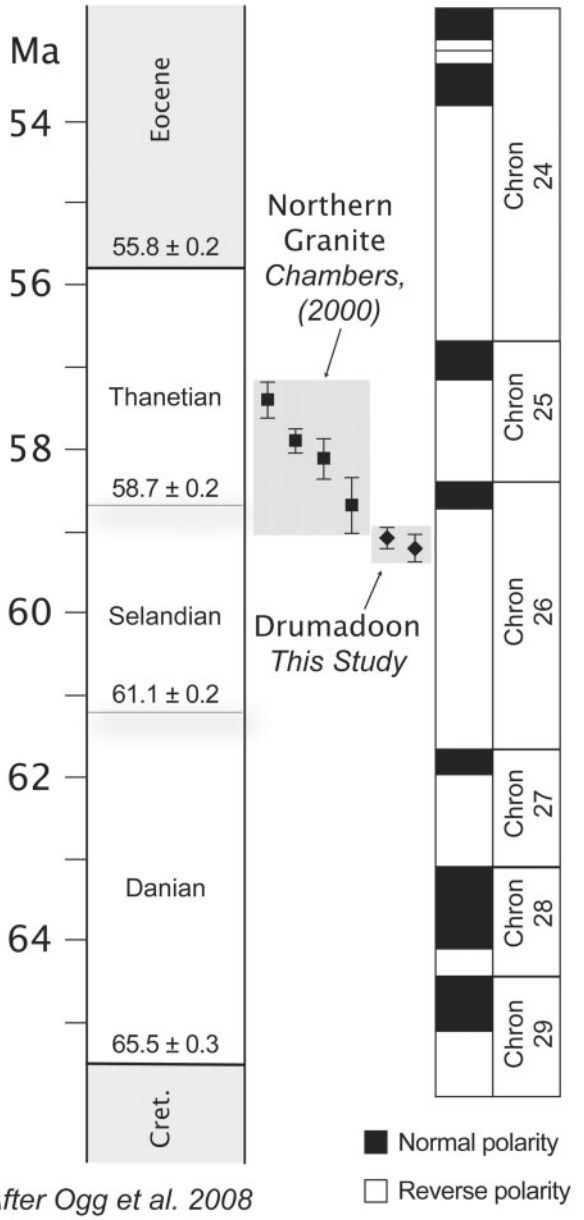

Fig. 14. Palaeomagnetic stratigraphy of the Palaeocene (Ogg *et al.*, 2008), with superimposed recent radiometric dates for the Drumadoon porphyritic rhyolite intrusions and the Northern Granite. Palaeomagnetic data were previously used to suggest that these intrusions all lay within chron 26n (Mussett *et al.*, 1987, 1989; Hodgson *et al.*, 1990).

26r–26n–25r for the Palaeogene igneous rocks of Arran. This would place both the Northern Granite and the porphyritic sills within the same normal anomaly (chron 26n), lying between the older Ailsa Craig–Holy Island alkaline magmatism (chron 26r) and the younger Central Complex (chron 25r). This study shows that this is not the case and that igneous activity must now span at least two periods of normal polarity.

Structure of the crust and the magma pathway

The Nd–Sr isotope data point towards major involvement of the Grampian terrane in the petrogenesis of the Drumadoon Intrusive Complex, even though the complex is located within the Midland Valley Terrane crustal block. Therefore, although the magmas originated at depth on the northern side of the Highland Boundary Fault, it is likely that they have crossed this boundary at some point during their evolution and ascent, probably during shallow-level emplacement, as all the data suggest the Grampian Terrane as the dominant crustal influence.

Gravimetric studies on the Highland Boundary Fault suggest a sub-vertical orientation, dipping very steeply to the NW (Dentith *et al.*, 1992). Given this geometry, the magma is unlikely to have followed a direct vertical pathway through the crust, but rather experienced an element of horizontal movement, not least during final shallow-level emplacement. Lateral transport of magma has been suggested at several other locations; for example, distances of ~10 km have been suggested for a silicic sill at Katmai, Alaska (Hildreth & Fierstein, 2000). Even larger amounts of lateral transport have been cited for basaltic systems. Distances up to 50 km have been envisaged for basaltic feeders to the Izu–Bonin arc volcanoes, Japan (Ishizuka *et al.*, 2008; Tamura *et al.*, 2009) and 300 km for feeders to the Columbia River system, USA (Wolff *et al.*, 2008). Shallow-level magma reservoirs are even considered to preferentially feed lateral intrusions and thus favour late-stage lateral transport (Grosfils, 2007).

As a suite, the porphyritic rhyolites on Arran (Kanaris-Sotiriou & Gibb, 1985), and those from Bute (Smellie, 1914, 1916; Buist, 1952), all crop out just south of the Highland Boundary Fault (Fig. 2). This suggests that the fault plane may have acted as an intrusion pathway along which the magma travelled, followed by intrusion into the footwall (Midland Valley Terrane) (Fig. 15). Intrusion into the footwall of faults has also been noted at the Skye igneous centre (Butler & Hutton, 1994).

An alternative crustal structure has been proposed by Strachan (2000), whereby some Grampian crust may have underthrust the Midland Valley Terrane during the Grampian Orogeny. This would result in a scenario whereby Dalradian rocks lie structurally below the rocks of the Midland Valley, meaning that magma could be contaminated by Grampian Terrane lithologies and still make a direct vertical traverse through the crust. Alternatively, the presence of isolated Dalradian-like crustal blocks within the MVT cannot be discounted. Such a scenario occurs in Northern Ireland, where the Tyrone Central Inlier, a metasedimentary block of Dalradian affinity, lies south of the inferred trace of the Highland Boundary Fault (Chew *et al.*, 2008). Although assimilation of

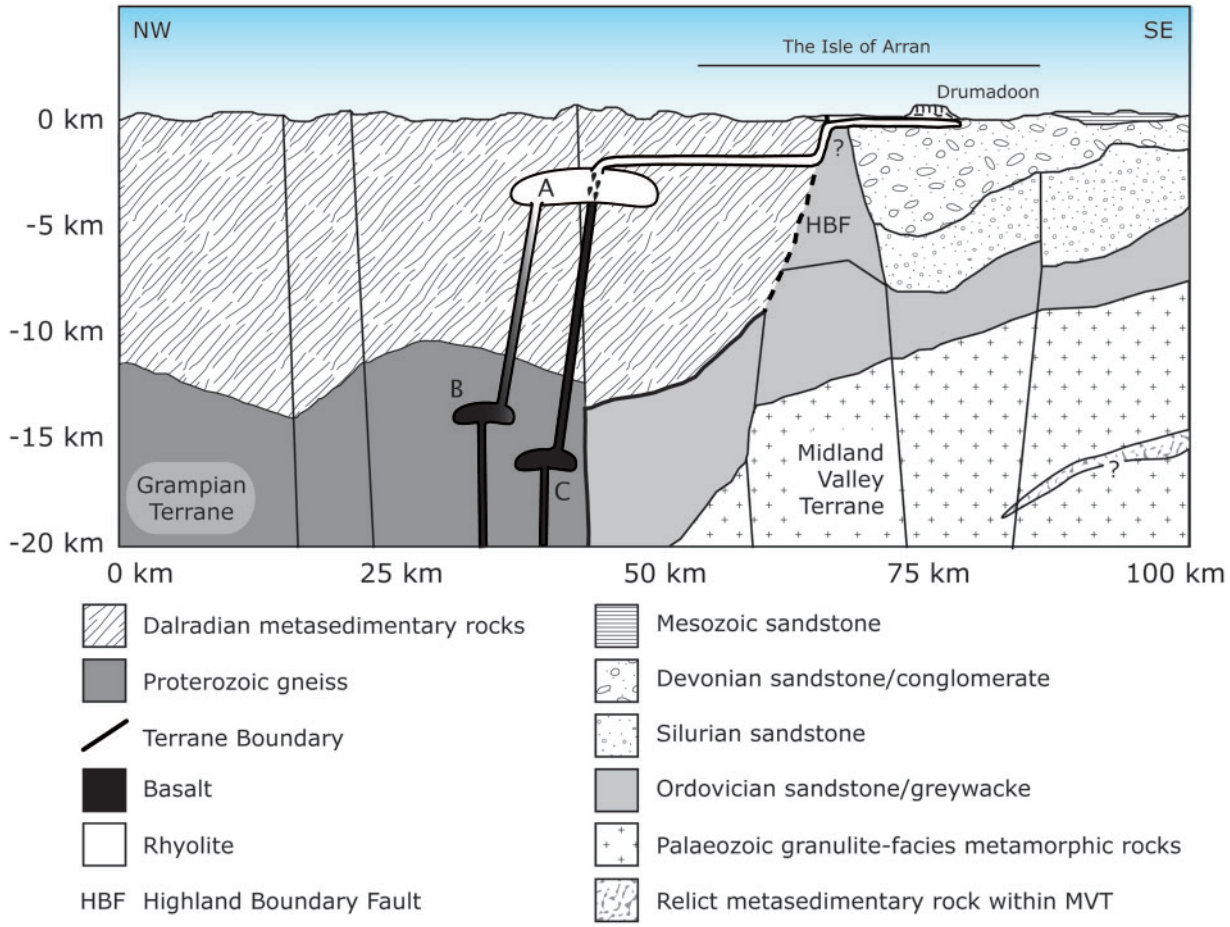

Fig. 15. Schematic diagram showing the intrusion pathways of both the rhyolitic and basaltic magmas that contributed to the Drumadoon Intrusive Complex. The rhyolite (A) is the product of assimilation and fractional crystallization of a basaltic magma (B) and has been contaminated in both the lower and upper crust. The Drumadoon basalt (C) shows a lower crustal influence only. These magmas (A and C) first met in the upper crust and mixed and mingled (see Fig. 13 for detailed view of high-level magma chamber events). They then intruded together across the terrane boundary, possibly exploiting the Highland Boundary Fault. The crustal cross-section is modified from fig. 1.11 of Trewin & Rollin (2002), which is based on observed gravity and magnetic anomalies. This profile represents a line of section ~55 km east of Arran.

Dalradian rocks within the Midland Valley Terrane may seem like a simpler emplacement scenario and would also explain the presence of metasedimentary xenoliths that have yielded Proterozoic bulk fraction U–Pb detrital zircon ages (Halliday *et al.*, 1984), we must consider how likely it is for this terrane to contain a significant thickness of Dalradian rock as well as southward-thinning Rhinns Complex-type lower crustal basement. Similarly, if the magmas were to take this route through the crust they would have had to travel through a significant portion of Midland Valley Terrane basement and Mesozoic–Palaeozoic sediments; however, we see no isotopic evidence of their involvement. Although the Midland Valley Terrane crust has a less radiogenic Sr isotopic signature than its Grampian Terrane equivalent, it might seem possible that the stronger Dalradian isotopic signature may have masked its influence, as assimilation of less radiogenic Midland Valley crust would simply reverse the trend (see Troll *et al.*, 2005). However, we have seen from geochemical modelling of AFC that the current isotopic ratio of the rhyolites suggests that they have neared the physical limit of assimilation of Dalradian crust (Reiners *et al.*, 1995). This implies that they have achieved the most radiogenic signature possible, implying therefore that their isotopic signature is unlikely to have been retrogressed as a result of incorporation of a third, less radiogenic, crustal end-member.

The only significant Midland Valley Terrane influence evident is the interaction of the margins of the sill with fluids within the surrounding sandstone country rocks. Here, heated fluids released from the heated country rocks are inferred to have leached several elements (TiO_2, V, Cr, etc.) from the marginal zones of the intrusions.

CONCLUSIONS

Within the Drumadoon Intrusive Complex, the exposed rock types show a typical BIPIP 'Bunsen–Daly gap' distribution (Bunsen, 1851; Daly, 1925), with strongly bimodal (basalt–rhyolite) compositions. Significantly, the intermediate compositions, although seemingly bridging the Bunsen–Daly gap, are not the product of fractional crystallization, but rather seem to be the result of mixing of basaltic and rhyolitic end-member compositions. The comparatively large volumes of felsic magma (porphyritic rhyolite) at Drumadoon are suggested to be the result of high levels of crustal assimilation during fractional crystallization of a basaltic parent magma.

It appears that the mixed basalt and rhyolite magmas initially had separate paths through the lower and mid-crust, and interacted only in the upper crust. The basaltic andesite shows lower crustal contamination by bulk mixing, but no upper crustal contamination is detectable. The porphyritic rhyolite is also likely to have been contaminated by small amounts of bulk mixing with the lower crust, but this was followed by large-scale AFC in the upper crust.

Within the upper crust, the basalt is likely to have encroached upon the crystallizing rhyolite body. On passing through the rhyolitic crystal mush, the basaltic magma mixed and mingled, forming the xenocryst-bearing basaltic andesite and the enclave-bearing rhyolite (Fig. 13). The basaltic andesite, being less viscous, would have flowed faster and formed the initial intrusion, lubricating the way for the viscous rhyolite. Work by Rubin (1995) suggests that it is difficult for granitic magmas to escape their source region, so lubrication by basaltic magma in the conduit may be crucial for transport of such magmas over longer distances (see Takeuchi & Nakamura, 2001). The available evidence suggests that the rising magmas crossed a major crustal boundary on emplacement and, taking into account the inclined nature of the Highland Boundary Fault, it is likely that they travelled laterally for a significant cumulative distance, perhaps as much as 30–40 km, during their traverse through the crust. Indeed, the fault zone itself may have been an important magma pathway (Fig. 15). Intrusions such as those at Drumadoon demonstrate that significant lateral transport of felsic magmas can occur, and care must be taken when assuming that such magmas have been contaminated by the crust into which they were intruded.

ACKNOWLEDGEMENTS

The authors would like to thank S. Daly and E. Holohan for stimulating discussion throughout the preparation of this paper. C. Nicholas and J.P. Morgan are thanked for discussions concerning the field relationships in the Drumadoon Igneous Complex. J. Geldmacher, K. Goodenough and R. MacDonald are thanked for detailed reviews, which greatly added to the final manuscript.

FUNDING

This research was made possible by an Irish Research Council for Science and Technology (IRCSET) postgraduate scholarship (F.C.M.) and a Science Foundation Ireland (SFI) basic research grant (V.R.T.).

REFERENCES

Abratis, M., Schmincke, H.-U. & Hansteen, T. H. (2002). Composition and evolution of submarine volcanic rocks from the central and western Canary Islands. *International Journal of Earth Sciences* **91**, 562–582.

Anderton, R. (1982). Dalradian deposition and the late Precambrian–Cambrian history of the N. Atlantic region: a review of the early evolution of the Iapetus Ocean. *Journal of the Geological Society, London* **139**, 421–431.

Annen, C. & Sparks, R. S. J. (2002). Effects of repetitive emplacement of basaltic intrusions on thermal evolution and melt generation in the crust. *Earth and Planetary Science Letters* **203**, 937–955.

Bamford, D., Nunn, K., Prodehl, C. & Jacob, B. (1977). LISPB; III, Upper crustal structure of northern Britain. *Journal of the Geological Society, London* **133**, 481–488.

Bell, B. R. & Williamson, I. T. (2002). Tertiary igneous activity. In: Trewin, N. H. (ed.) *The Geology of Scotland*, 4th edn. London: Geological Society, pp. 371–407.

British Geological Survey*Bedrock geology UK North, 1:625 000*. Keyworth, Nottingham: British Geological Survey.

Brown, J. W. (1929). Dykes and associated intrusions of the Island of Bute. *Transactions of the Geological Society of Glasgow* **18**, 388–419.

Bryan, W. B., Finger, L. W. & Chayes, F. (1969). Estimating proportions in petrographic mixing equations by least-squares approximation. *Science* **163**, 926–927.

Buist, D. S. (1952). A contribution to the petrochemistry and petrogenesis of the composite sill of South Bute. *Transactions of the Edinburgh Geological Society* **15**, 52–68.

Buist, D. S., Ineson, P. R. & Mitchell, J. G. (1979). Isotopic age determinations on the composite sill and associated olivine dolerite, South Bute. *Scottish Journal of Geology* **15**, 257–262.

Bunsen, R. W. (1851). Über die Processe der vulkanischen Gesteinsbildungen Islands. *Annalen der Physik und Chemie* **83**, 197–272.

Butler, R. W. H. & Hutton, D. H. W. (1994). Basin structure and Tertiary magmatism on Skye, NW Scotland. *Journal of the Geological Society, London* **151**, 931–944.

Campbell, I. H. & Griffiths, R. W. (1990). Implications of mantle plume structure for the evolution of flood basalts. *Earth and Planetary Science Letters* **99**, 79–93.

Chambers, L. M. (2000). Age and duration of the British Tertiary Igneous Province: implications for the development of the ancestral Iceland plume. Ph.D. thesis, University of Edinburgh.

Chambers, L. M. & Pringle, M. S. (2001). Age and duration of activity at the Isle of Mull Tertiary igneous centre, Scotland, and confirmation of the existence of subchrons during Anomaly 26r. *Earth and Planetary Science Letters* **193**, 333–345.

Chew, D. M. (2003). Structural and stratigraphic relationships across the continuation of the Highland Boundary Fault in western Ireland. *Geological Magazine* **140**, 73–85.

Chew, D. M., Flowerdew, M. J., Page, L. M., Crowley, Q. G., J. S., D. & Cooper, M.J. (2008). The tectonothermal evolution and provenance of the Tyrone Central Inlier, Ireland: Grampian imbrication of an outboard Laurentian microcontinent? *Journal of the Geological Society, London* **165**, 675–685.

Dagley, P., Mussett, A. E., Wilson, R. L. & Hall, J. M. (1978). The British Tertiary igneous province; palaeomagnetism of the Arran dykes. *Geophysical Journal of the Royal Astronomical Society* **54**, 75–91.

Dalrymple, G. B. & Lamphere, M. A. (1972). $^{40}Ar/^{39}Ar$ technique of K–Ar dating: a comparison with the conventional technique. *Earth and Planetary Science Letters* **12**, 300–308.

Daly, J. S., Muir, R. J. & Cliff, R. A. (1991). A precise U–Pb zircon age for the Inishtrahull syenite gneiss, County Donegal, Ireland. *Journal of the Geological Society, London* **148**, 639–642.

Daly, R. A. (1925). The Geology of Ascension Island. *Proceedings of the American Academy of Arts and Science* **60**, 1–80.

Deniel, C. & Pin, C. (2001). Single-stage method for the simultaneous isolation of lead and strontium from silicate samples for isotopic measurements. *Analytica Chimica Acta* **426**, 95–103.

Dentith, M. C., Trench, A. & Bluck, B. J. (1992). Geophysical constraints on the nature of the Highland Boundary Fault Zone in western Scotland. *Geological Magazine* **129**, 411–419.

DePaolo, D. J. (1981). Trace element and isotopic effects of combined wallrock assimilation and fractional crystallisation. *Earth and Planetary Science Letters* **53**, 189–202.

Dewey, J. F. (2005). Orogeny can be very short. *Proceedings of the National Academy of Sciences of the USA* **102**, 15286–15293.

Dickin, A. P. (1992). Evidence for an Early Proterozoic crustal province in the North Atlantic region. *Journal of the Geological Society, London* **149**, 483–486.

Dickin, A. P. (1994). Nd isotope chemistry of Tertiary igneous rocks from Arran, Scotland; implications for magma evolution and crustal structure. *Geological Magazine* **131**, 329–333.

Dickin, A. P. & Bowes, D. R. (1991). Isotopic evidence for the extent of early Proterozoic basement in Scotland and Northwest Ireland. *Geological Magazine* **128**, 385–388.

Dickin, A. P. & Durant, G. P. (2002). The Blackstones Bank igneous complex: geochemistry and crustal context of a submerged Tertiary igneous centre in the Scottish Hebrides. *Geological Magazine* **139**, 199–207.

Dickin, A. P., Moorbath, S. & Welke, H. J. (1981). Isotope, trace element and major element geochemistry of Tertiary igneous rocks, Isle of Arran, Scotland. *Transactions of the Royal Society of Edinburgh: Earth Sciences* **72**, 159–170.

Dickin, A. P., Brown, J. L., Thompson, R. N., Halliday, A. N., Morrison, M. A., Hutchison, R. & O'Hara, M. J. (1984). Crustal contamination and the granite problem in the British Tertiary Volcanic Province. *Philosophical Transactions of the Royal Society of London, Series A* **310**, 755–780.

Duffield, W. A. & Ruiz, J. (1998). A model that helps explain Sr-isotope disequilibrium between feldspar phenocrysts and melt in large-volume silicic magma systems. *Journal of Volcanology and Geothermal Research* **87**, 7–13.

Eldholm, O. & Grue, K. (1994). North Atlantic volcanic margins: dimensions and production rates. *Journal of Geophysical Research* **99**, 2955–2968.

Ellam, R. M. & Stuart, F. M. (2000). The sub-lithospheric source of North Atlantic basalts; evidence for, and significance of, a common end-member. *Journal of Petrology* **41**, 919–932.

Emeleus, C. H. (1962). The porphyritic felsite of the Tertiary ring complex of Slieve Gullion, Co. Armagh. *Proceedings of the Royal Irish Academy* **62**, 55–76.

Emeleus, C. H. & Bell, B. R. (2005). *British regional geology: the Palaeogene volcanic districts of Scotland*. Keyworth, Nottingham: British Geological Survey, 214 p.

England, R. W. (1992). The genesis, ascent, and emplacement of the Northern Arran Granite, Scotland; implications for granitic diapirism. *Geological Society of America Bulletin* **104**, 606–614.

Evans, A. L., Fitch, F. J. & Miller, J. A. (1973). Potassium–argon age determinations on some British Tertiary igneous rocks. *Journal of the Geological Society, London* **129**, 419–443.

Faure, G. (2001). Interlaboratory Sr-isotope Standards. In: Faure, G. (ed.) *Origin of Igneous Rocks: the Isotopic Evidence*. Berlin: Springer, 8 p.

Fitches, W. R., Muir, R. J., Maltman, A. J. & Bentley, M. R. (1990). Is the Colonsay–west Islay block of SW Scotland an allochthonous terrane? Evidence from Dalradian tillite clasts. *Journal of the Geological Society, London* **147**, 417–420.

Frost, C. D. & O'Nions, R. K. (1985). Caledonian magma genesis and crustal recycling. *Journal of Petrology* **26**, 515–544.

Gamble, J. A., Meighan, I. G. & McCormick, A. G. (1992). The petrogenesis of Tertiary microgranites and granophyres from the Slieve Gullion central complex, NE Ireland. *Journal of the Geological Society, London* **149**, 93–106.

Geldmacher, J., Haase, K. M., Devey, C. W. & Garbe-Schoenberg, C. D. (1998). The petrogenesis of Tertiary cone-sheets in Ardnamurchan, NW Scotland; petrological and geochemical constraints on crustal contamination and partial melting. *Contributions to Mineralogy and Petrology* **131**, 196–209.

Geldmacher, J., Troll, V. R., Emeleus, C. H. & Donaldson, C. H. (2002). Pb-isotope evidence for contrasting crustal contamination of primitive to evolved magmas from Ardnamurchan and Rum; implications for the structure of the underlying crust. *Scottish Journal of Geology* **38**, 55–61.

Gradstein, F. M., Ogg, J. G. & Smith, A. G. (eds) (2004). *A Geological Time Scale*. Cambridge: Cambridge University Press, 610 p.

Graham, A. M. & Upton, B. G. J. (1978). Gneisses in diatremes, Scottish Midland Valley; petrology and tectonic implications. *Journal of the Geological Society, London* **135**, 219–228.

Grosfils, E. B. (2007). Magma reservoir failure on the terrestrial planets: Assessing the importance of gravitational loading in simple elastic models. *Journal of Volcanology and Geothermal Research* **166**, 47–75.

Hall, J., Brewer, J. A., Matthews, D. H. & Warner, M. R. (1984). Crustal structure across the Caledonides from the 'WINCH' seismic reflection profile; influences on the evolution of the Midland Valley of Scotland. *Transactions of the Royal Society of Edinburgh: Earth Sciences* **75**, 97–109.

Halliday, A. N., Aftalion, M., Upton, B. G. J., Aspen, P. & Jocelyn, J. (1984). U–Pb isotopic ages from a granulite-facies xenolith from Partan Craig in the Midland Valley of Scotland. *Transactions of the Royal Society of Edinburgh* **75**, 71–74.

Halliday, A. N., Dickin, A. P., Hunter, R. N., Davies, G. R., Dempster, T. J., Hamilton, P. J. & Upton, B. G. J. (1993). Formation and composition of the lower continental crust; evidence from Scottish xenolith suites. *Journal of Geophysical Research* **98**, 581–607.

Harrison, J. V. (1925). The geology of a composite intrusion at Bennan, South Arran. *Transactions of the Geological Society of Glasgow* **17**, 173–180.

Hildreth, W. & Fierstein, J. (2000). Katmai volcanic cluster and the great eruption of 1912. *Geological Society of America Bulletin* **112**, 1594–1620.

Hitchen, K., Morton, A. C., Mearns, E. W., Whitehouse, M. & Stoker, M. S. (1997). Geological implications from geochemical and isotopic studies of Upper Cretaceous and Lower Tertiary igneous rocks around the northern Rockall Trough. *Journal of the Geological Society, London* **154**, 517–521.

Hodgson, B. D., Dagley, P. & Mussett, A. E. (1990). Magnetostratigraphy of the Tertiary igneous rocks of Arran. *Scottish Journal of Geology* **26**, 99–118.

Holbrook, W. S., Larsen, H. C., Korenaga, J., Dahl-Jensen, T., Reid, I. D., Kelemen, P. H., Hopper, P. R., Kent, G. M., Lizzaralde, D., Bernstein, S. & Detrick, R. S. (2001). Mantle thermal structure and active upwelling during continental breakup in the North Atlantic. *Earth and Planetary Science Letters* **190**, 251–266.

Hynes, A. (1980). Carbonization and mobility of Ti, Y and Zr in Ascot Formation metabasalts, SE Quebec. *Contributions to Mineralogy and Petrology* **75**, 79–87.

Hyslop, E. K., Gillanders, R. J., Hill, P. G. & Fakes, R. D. (1999). Rare-earth-bearing minerals fergusonite and gadolinite from the Arran granite. *Scottish Journal of Geology* **35**, 65–69.

Ishizuka, O., Geshi, N., Itoh, J., Kawanabe, Y. & TuZino, T. (2008). The magmatic plumbing of the submarine Hachijo NW volcanic chain, Hachijojima, Japan: Long-distance magma transport? *Journal of Geophysical Research* **113**, B08S08, doi:10.1029/2007JB005325.

Judd, J. W. (1893). On composite dykes in Arran. *Quarterly Journal of the Geological Society of London* **49**, 536–565.

Kanaris-Sotiriou, R. & Gibb, F. G. F. (1985). Hybridization and the petrogenesis of composite intrusions; the dyke at An Cumhann, Isle of Arran, Scotland. *Geological Magazine* **122**, 361–372.

Kerr, A. C. & Kempton, P. D. (1995). Crustal assimilation during turbulent magma ascent (ATA); new isotopic evidence from Mull Tertiary lava succession, N. W. Scotland. *Contributions to Mineralogy and Petrology* **119**, 142–154.

Kerr, A. C., Kent, R. W., Thomson, B. A., Seedhouse, J. K. & Donaldson, C. H. (1999). Geochemical evolution of the Tertiary Mull volcano, western Scotland. *Journal of Petrology* **40**, 873–908.

King, B. C. (1955). The Ard Bheinn area of the central igneous complex of Arran. *Quarterly Journal of the Geological Society of London* **110**, 323–355.

Langmuir, C. H., Vocke, R. D., Hansan, G. N. & Hart, S. R. (1978). A general mixing equation with applications to Icelandic basalts. *Earth and Planetary Science Letters* **37**, 380–392.

MacDonald, J. G. & Herriot, A. (1983). *Macgregor's Excursion Guide to the Geology of Arran*. Glasgow: Geological Society of Glasgow, 210 p.

Marcantonio, F., Dickin, A. P., McNutt, R. H. & Heaman, L. M. (1988). A 1,800-million-year-old Proterozoic gneiss terrane in Islay with implications for the crustal structure and evolution of Britain. *Nature* **335**, 62–64.

Marshall, L. A. & Sparks, R. S. J. (1984). Origin of some mixed-magma and net-veined ring intrusions. *Journal of the Geological Society, London* **141**, 171–182.

McDonnell, S., Troll, V. R., Emeleus, C. H., Meighan, I. G., Brock, D. & Gould, R. J. (2004). Intrusive history of the Slieve Gullion ring dyke, Ireland: implications for the internal structure of silicic subcaldera magma chambers. *Mineralogical Magazine* **68**, 725–738.

Meighan, I. G. (1979). The acid igneous rocks of the British Tertiary province. *Bulletin of the Geological Survey of Great Britain* **70**, 7–8 and 10–22.

Meighan, I. G., Gibson, D. & Hood, D. N. (1984). Some aspects of Tertiary acid magmatism in NE Ireland. *Mineralogical Magazine* **48**, 351–363.

Meyer, R., van Wijk, J. & Gernigon, L. (2007). North Atlantic Igneous Province: a review of models for its formation. In: Foulger, G. R. & Jurdy, D. M. (eds) *Plates, Plumes, and Planetary Processes. Geological Society of America, Special Papers* **430**, 525–552.

Mussett, A. E., Dagley, P., Hodgson, B. & Skelhorn, R. R. (1987). Palaeomagnetism and age of the quartz-porphyry intrusions, Isle of Arran. *Scottish Journal of Geology* **23**, 9–22.

Mussett, A. E., Dagley, P. & Skelhorn, R. R. (1989). Further evidence for a single polarity and a common source for the quartz-porphyry intrusions of the Arran area. *Scottish Journal of Geology* **25**, 353–359.

Nabelek, P. I. (2007). Fluid evolution and kinetics of metamorphic reactions in calc-silicate contact aureoles—From H_2O to CO_2 and back. *Geology* **35**, 927–930.

Ogg, J. G., Ogg, G. & Gradstein, F. M. (2008). *The Concise Geologic Time Scale*. Cambridge: Cambridge University Press, 177 p.

Olive, V., Ellam, R. M. & Wilson, L. (2001). A protocol for the determination of the rare earth elements at picomole level in rocks by ICP-MS: results on geological reference materials USGS PCC-1 and DTS-1. *Geostandards Newsletter* **25**, 219–228.

Palacz, Z. A. (1985). Sr–Nd–Pb isotopic evidence for crustal contamination in the Rhum Intrusion. *Earth and Planetary Science Letters* **74**, 35–44.

Paquet, F., Dauteuil, O., Hallot, E. & Moreau, F. (2007). Tectonics and magma dynamics coupling in a dyke swarm of Iceland. *Journal of Structural Geology* **29**, 1477–1493.

Pearce, J. A. & Cann, J. R. (1973). Tectonic setting of basic volcanic rocks determined using trace element analyses. *Earth and Planetary Science Letters* **19**, 290–300.

Pin, C. & Santos Zaldegui, J. F. (1997). Sequential separation of light rare-earth elements, thorium and uranium by miniaturized extraction chromatography: Application to isotopic analyses of silicate rocks. *Analytica Chimica Acta* **339**, 79–89.

Raczek, I., Stoll, B., Hofmann, A. W. & Jochum, K. P. (2001). High-precision trace element data for the USGS Reference Materials BCR-1, BCR-2, BHVO-1, AGV-1, AGV-2, DTS-1, DTS-2, GSP-1 and GPS-2 by ID-TIMS and MIC-SSMS. *Geostandards Newsletter* **25**, 77–86.

Reiners, P. W., Nelson, B. K. & Ghiorso, M. S. (1995). Assimilation of felsic crust by basaltic magma: thermal limits and extents of crustal contamination of mantle-derived magmas. *Geology* **23**, 563–566.

Richards, M. A., Duncan, R. A. & Courtillot, V. E. (1989). Flood basalts and hot-spot tracks: plume heads and tails. *Science* **246**, 103–107.

Rubin, A. M. (1995). Getting granite dikes out of the source region. *Journal of Geophysical Research* **100**, 5911–5929.

Saunders, A. D., Norry, M. J. & Tarney, J. (1988). Origin of MORB and chemically-depleted mantle reservoirs; trace element constraints. *Journal of Petrology* **29**, 415–445.

Smallwood, J. R. & White, R. S. (2002). Ridge–plume interaction in the North Atlantic and its influence on continental breakup and seafloor spreading. In: Jolley, D. W. & Bell, B. R. (eds) *The North Atlantic Igneous Province: Stratigraphy, Tectonic, Volcanic and Magmatic Processes. Geological Society, London, Special Publications* **197**, 15–37.

Smellie, W. R. (1914). The Tertiary composite sill of South Bute. *Transactions of the Geological Society of Glasgow* **15**, 121–139.

Smellie, W. R. (1916). The igneous rocks of Bute. *Transactions of the Geological Society of Glasgow* **15**, 334–373.

Sparks, R. S. J. (1988). Petrology and geochemistry of the Loch Ba ring-dyke, Mull (N.W.) Scotland: an example of the extreme differentiation of tholeiitic magmas. *Contributions to Mineralogy and Petrology* **100**, 446–461.

Speight, J. M., Skelhorn, R. R., Sloan, T. & Knaap, R. J. (1982). The dyke swarms of Scotland. In: Sutherland, D. S. (ed.) *Igneous Rocks of the British Isles*. Chicester: John Wiley, pp. 449–459.

Stevenson, C. T. E., Owens, W. H., Hutton, D. H. W., Hood, D. N. & Meighan, I. G. (2007). Laccolithic, as opposed to cauldron subsidence, emplacement of the Eastern Mourne Pluton, N. Ireland; evidence from anisotropy of magnetic susceptibility. *Journal of the Geological Society, London* **164**, 99–110.

Storey, M., Duncan, R. A. & Tegner, C. (2007). Timing and duration of volcanism in the North Atlantic Igneous Province: Implications for geodynamics and links to the Iceland hotspot. *Chemical Geology* **241**, 264–281.

Strachan, R. A. (2000). The Grampian Orogeny: Mid-Ordovician arc–continent collision along the Laurentian margin of Iapetus. In: Woodcock, N. H. & Strachan, R. A. (eds) *Geological History of Britain and Ireland*. Oxford: Blackwell, pp. 88–106.

Takeuchi, S. & Nakamura, M. (2001). Role of precursory less-viscous mixed magma in the eruption of phenocryst-rich magma: evidence from the Hokkaido–Komagatake 1929 eruption. *Bulletin of Volcanology* **63**, 365–376.

Tamura, Y., Gill, J. B., Tollstrup, D., Kawabata, H., Shukuno, H., Chang, Q., Miyazaki, T., Takahashi, T., Hirahara, Y., Kodaira, S., Ishizuka, O., Suzuki, T., Kido, Y., Fiske, R. S. & Tatsumi, Y. (2009). Silicic magmas in the Izu–Bonin oceanic arc and implications for crustal evolution. *Journal of Petrology* **50**, 685–723.

Tanner, G. (2008). Tectonic significance of the Highland Boundary Fault, Scotland. *Journal of the Geological Society, London* **165**, 915–921.

Tantrigoda, D. A. (1999). Interpretation of magnetic anomalies over the Isle of Arran. *Scottish Journal of Geology* **35**, 51–55.

Thompson, R. N. (1969). Tertiary granites and associated rocks of the Marsco area, Isle of Skye. *Quarterly Journal of the Geological Society of London* **124**, 349–385.

Thompson, R. N., Morrison, M. A., Dickin, A. P., Gibson, I. L. & Harmon, R. S. (1986). Two contrasting styles of interaction between basic magmas and continental crust in the British Tertiary volcanic province. *Journal of Geophysical Research* **91(B6)**, 5985–5998.

Trewin, N. H. (ed.) (2002). *The Geology of Scotland*. London: Geological Society, 576 p.

Trewin, N. H. & Rollin, K. E. (2002). Geological history and structure of Scotland. In: Trewin, N. H. (ed.) *The Geology of Scotland*. London: Geological Society, pp. 1–25.

Troll, V. R., Donaldson, C. H. & Emeleus, C. H. (2004). Pre-eruptive magma mixing in ash-flow deposits of the Tertiary Rum igneous centre, Scotland. *Contributions to Mineralogy and Petrology* **147**, 722–739.

Troll, V. R., Chadwick, J. P., Ellam, R. M., McDonnell, S., Emeleus, C. H. & Meighan, I. G. (2005). Sr and Nd isotope evidence for successive crustal contamination of Slieve Gullion ring-dyke magmas, Co. Armagh, Ireland. *Geological Magazine* **142**, 659–668.

Tyrrell, G. W. (1928). *The Geology of Arran*. Edinburgh: HMSO.

Upton, B. G. J. (1988). History of Tertiary igneous activity in the N Atlantic borderlands. In: Morton, A. C. & Parson, L. M. (eds) *Early Tertiary Volcanism and the Opening of the NE Atlantic. Geological Society, London, Special Publications* **39**, 429–453.

White, R. S. & McKenzie, D. P. (1989). Magmatism at rift zones: the generation of volcanic continental margins and flood basalts. *Journal of Geophysical Research* **94**, 7685–7729.

Wolff, J. A., Ramos, F. C., Hart, G. L., Patterson, J. D. & Brandon, A. D. (2008). Columbia River flood basalts from a centralized crustal magmatic system. *Nature Geoscience* **1**, 177–180.

Yoder, H. S. (1973). Contemporaneous basaltic and rhyolitic magmas. *American Mineralogist* **58**, 153–171.